BILINGUAL PUBLISHING CO.
Pioneer of Global Academics Since 1984

Organic Polymer Material Research

Volume 3 | Issue 2 | December 2021 | ISSN 2661-3875（Online）

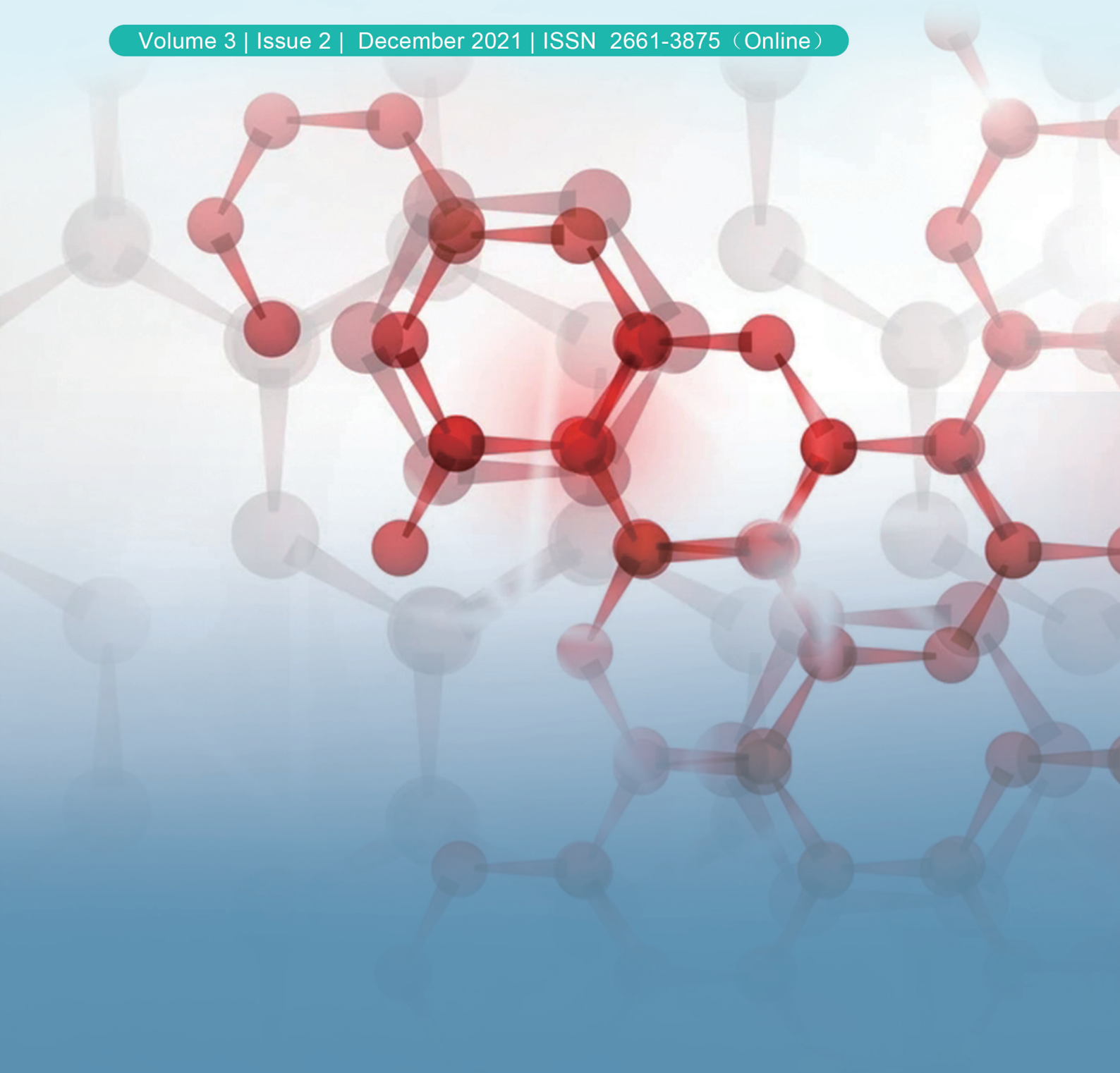

Volume 3 Issue 2 • December 2021 • ISSN 2661-3875 (Online)

Organic Polymer Material Research

BILINGUAL PUBLISHING CO.
Pioneer of Global Academics Since 1984

BILINGUAL PUBLISHING CO.
Pioneer of Global Academics Since 1984

Volume 3 | Issue 2 | December 2021 | Page1-25
Organic Polymer Material Research

Contents

Editorial

Articles

Review

BILINGUAL PUBLISHING CO.
Pioneer of Global Academics Since 1984

Organic Polymer Material Research
https://ojs.bilpublishing.com/index.php/opmr

ARTICLE

Extraction of Dyes from Sunflower Petal and Their Fourier Transform Infrared Characterization

Gboyega Oluwaseun Oyeleke[1*] Ibraheem Abimbade Abdulazeez[2] Ajisola Agnes Adebisi[2] Kehinde Nasiru Oyekanmi[2] Segun Olaitan Akinbode[2]

1. Department of Science Laboratory Technology, Osun State Polytechnic, Iree, Nigeria
2. Department of Applied Science, Osun State Polytechnic, Iree, Nigeria

ARTICLE INFO

Article history
Received: 17 November 2020
Accepted: 21 June 2021
Published Online: 5 January 2022

Keywords:
Sunflower
Petal
Solvents
Dye extract
FT-IR
Functional group
Characterization

ABSTRACT

Three solvents of different polarities (water, methanol and 1% NaOH solution) were used to extract dyes that produced different shades from dried sunflower (*Helianthus annuus*) petal. The extraction procedures using different solvent types were carried out separately. The dye extracts were thereafter subjected to Fourier Transform Infrared Spectrometry (FT-IR) analysis for characterization in terms of functional groups. The intensities of the extracted dyes on the shade of colours obtained on pieces of cotton material varied from yellow in methanolic extract to light yellow in aqueous and black in 1% NaOH solution extracts. The results obtained from the FT-IR analysis revealed the presence of several useful functional groups such as N-H, C=H, O-H and C=O in the extracts.

1. Introduction

Chemical processes are influenced by the properties of solvents in which they are carried out [1]. It was reported by [2,3] that as the polarity of a solvent increase, its solubility and ability to solvate will decrease. Solvent effects have been associated with hydrogen bonding which assists electron migration in the molecules and stabilization of preferred structures [4]. Factors that determine solubility at either end of the polarity scale are complex and depend on combination of hydrogen donor acceptor strength and dipolar character. A strong solvent-solute interaction makes the process of solvation more favourable. Studies on effects of solvents of varying polarity on the reactivity and solubility of compounds have been reported [2,3,5,6].

**Corresponding Author:*
Gboyega Oluwaseun Oyeleke,
Department of Science Laboratory Technology, Osun State Polytechnic, Iree, Nigeria;
Email: gooyeleke@gmail.com

DOI: https://doi.org/10.30564/opmr.v3i2.2586

The decline in extracting and using of natural dyes has been resuscitated due to the fact that they are eco-friendly, biodegradable, non toxic, non allergic [7,8] and do not stain other fabrics when bleeding [9]. Natural dyes are colourants obtained from different natural sources without any synthesizing. It includes all the dyes derived from different natural sources such as plants, animals and minerals [8]. Uddin *et al.* [10] reported that majority of vegetative origin such as roots, berries, barks, leaves, wood and other biological sources like fungi and lichens. Extraction of dye from different plant sources have also been documented by several other workers [11-13].

Sunflower (*Helianthus annuus*) is a common plant in Nigeria. It is a tall annual plant that can grow to a height of 300 cm or more in some species. They bear one or more wide flower head with yellow ray florets at the outside and yellow or maroon disc florets inside. The plant is perceived to be a drought tolerant crop as its roots can take up water at depth not reached by other crops. The use of various plant parts as dye or colouring matter can be expanded by understanding its solubility in different solvents. Different coloured extracts from a particular plant source can be achieved depending on extraction methods [14].

Numerous scientific methodologies such as ultra violet (UV) -visible, fourier transform infra red (FT-IR) and gas chromatography – mass spectrometry (GC-MS) methods among others are available to analyse the effects of the solvent treatments on the characteristics of organic compounds. FT-IR spectroscopic analysis is however one of the most common and perhaps the most powerful technique for identifying the type of functional groups in biological samples and offers high speed quantitative analysis without consumption or destruction of the sample [15]. Its structural identification is based on the interaction of atoms with infrared radiation. When infrared radiation interacts with an organic compound, certain frequencies of energy are absorbed or reflected and these frequencies are determined by the functional groups present in the substance. IR method can be used singly or in combination with other techniques of instrumental analysis to identify the actual chemical composition of a material [16]. Several workers [17-21] reported the use of FT-IR for bioactive ingredients determination in different plant extracts. Reports on the dye extracts from sunflower petal using different solvents are relatively unavailable in the searched literature, therefore this research aimed at extracting dyes from sunflower petal using methanol, water and 1% NaOH solution. The extracted dyes are to be characterized using fourier transform infrared spectroscopy to determine the functional groups present in each of the extracts in order to ascertain if they are good dyes or otherwise.

2. Materials and Methods

2.1 Sample Collection

The sunflower (*Helianthus annuus*) petals were collected behind the Directorate of Entrepreneurship Education Centre of Osun State Polytechnic, Iree in the month of October, 2020. After collection, attached leaf and sepals were separated from the petals. The sample was identified as *Helianthus annuus* petals by Mr Akinro Ebenezer Babatope (Biology unit) of the Department of Science Laboratory Technology, Osun State Polytechnic, Iree, Nigeria.

2.2 Sample Preparation

The sunflower petals collected were air dried at room temperature for 14 days, sorted to further remove unwanted parts, pulverised using an electric Laboratory blender, passed through a 2 mm sieve and stored in a polythene bag kept over silica gel in a dessicator and ready for further analysis.

2.3 Extraction of Dye

Extraction of the dye was done using three different solvents; water, 1% NaOH, and analytical grade methanol.

2.3.1 Aqueous Extraction

The extraction of dye using water was carried out using the following procedures 20 g of the prepared sample was weighed and 400 mL of deionised distilled water was added over a water bath for 60 min at 60 ^{o}C. The mixture was removed from the water bath and left for 48 h after which it was filtered through Whatman No. 1 filter paper. Another 200 mL of deionised water was added to the residue and left for 24 h before it was filtered as above. The residue was further washed continuously with two more portions of 50 mL deionised distilled water for adequate extraction. The supernatants was pooled together, evaporated at 60 ^{o}C until the volume was reduced to 100 mL and stored in air tight bottles ready for further analysis.

2.3.2 1% NaOH Extraction

The extraction of dye using 1% NaOH solution was carried out using the following procedures. 20 g of the prepared sample was weighed into a 500 mL conical flask; 50 mL of the solvent was added and kept for 3 days. The extracts were filtered using Whatman No. 1 filter paper

and the supernatant was collected. The residue was further extracted two more times using 25 mL of the extracting solvent with 3 days' interval for each extraction. Each of the supernatants was separately pooled together and stored in air tight bottles ready for further analysis.

2.3.3 Methanolic Extraction

The dye extractions using methanol was done with a little modification to Ashokkumar and Ramaswamy [17] methods. 20 g of the sample was weighed into a 500 mL conical flasks; 150 mL of the solvents was added and kept for 3 days. The extract was thereafter filtered using Whatman No. 1 filter paper and the supernatants collected. The residue was further extracted two more times as above with 3 days' interval. The supernatants was pooled together, evaporated on a thermostatic water bath at 40 ^{o}C until the volume was reduced to 100 mL and stored in air tight bottle ready for further analysis.

2.3.4 FT-IR Analysis

The FT-IR analysis was carried out by encapsulating 30 mg of each extracts into 300 mg of KBr (dried at 80^{o}C for 24 h to completely remove moisture) pellet of spectroscopic grade purity using a small agate mortar until the sample was completely mixed with the KBr powder to produce a translucent sample discs. IR spectra regions and peaks produced were recorded at room temperature on Perkin-Elmer Fourier Transform spectrometer (RX model) Norwalk, CT, USA for the sample in each solvent with a scan range between 4000 - 400 cm^{-1} (1% NaOH), 4000 - 450 cm^{-1} (methanol) and 4000 - 500 cm^{-1} (water).

3. Results and Discussion

Table 1. Observed colours on the piece of cloth dyed with the different extracts

xtract	Piece of cloth	Colour observed
Methanol	Cotton material	Yellow
Aqueous	Cotton material	Light yellow
1% NaOH	Cotton material	Black

The visually observation of colours on the pieces of cotton materials dyed with the different extracts from the sunflower petal are shown in Table 1. The intensities of the shade of the colours obtained varied from yellow in methanolic extract to light yellow in aqueous and black in 1% NaOH extracts. The variation in colour intensities of the dyed materials may be adduced to type of solvents used and the observed different functional groups such as N-H, C=H, O-H and C=O groups in the extract. This is at variance with the report on dye extracted from *Rothmannia whitfieldii* where alkali extraction gave a deep brown colour liquid and aqueous extraction gave a black colour liquid [14].

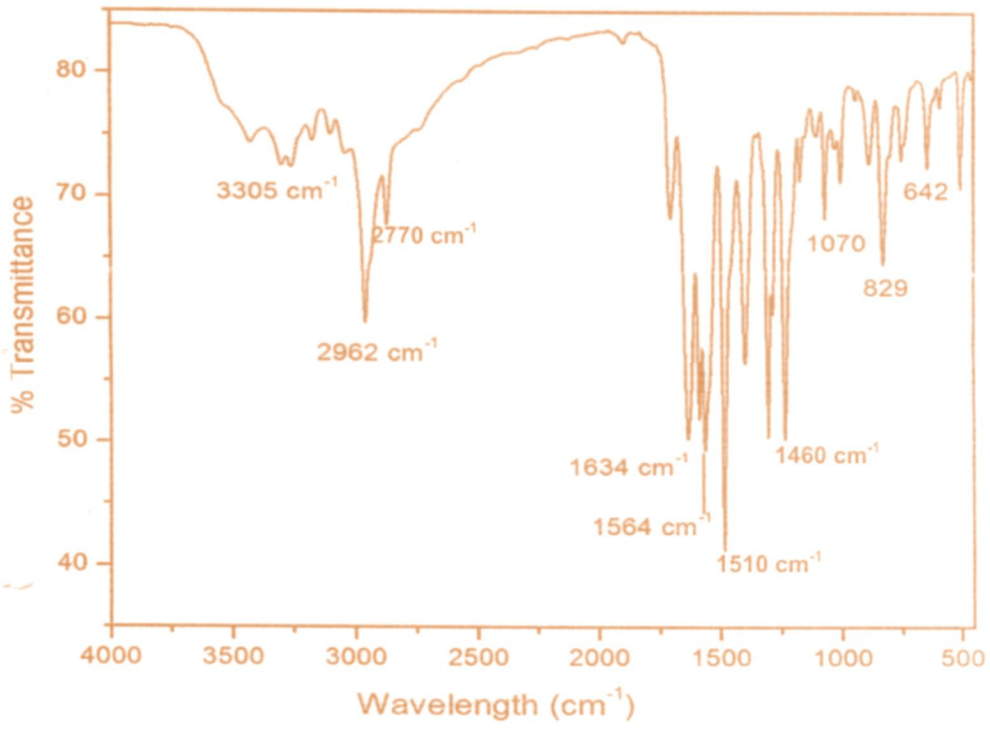

Figure 1. FT-IR spectral of aqueous dye extract

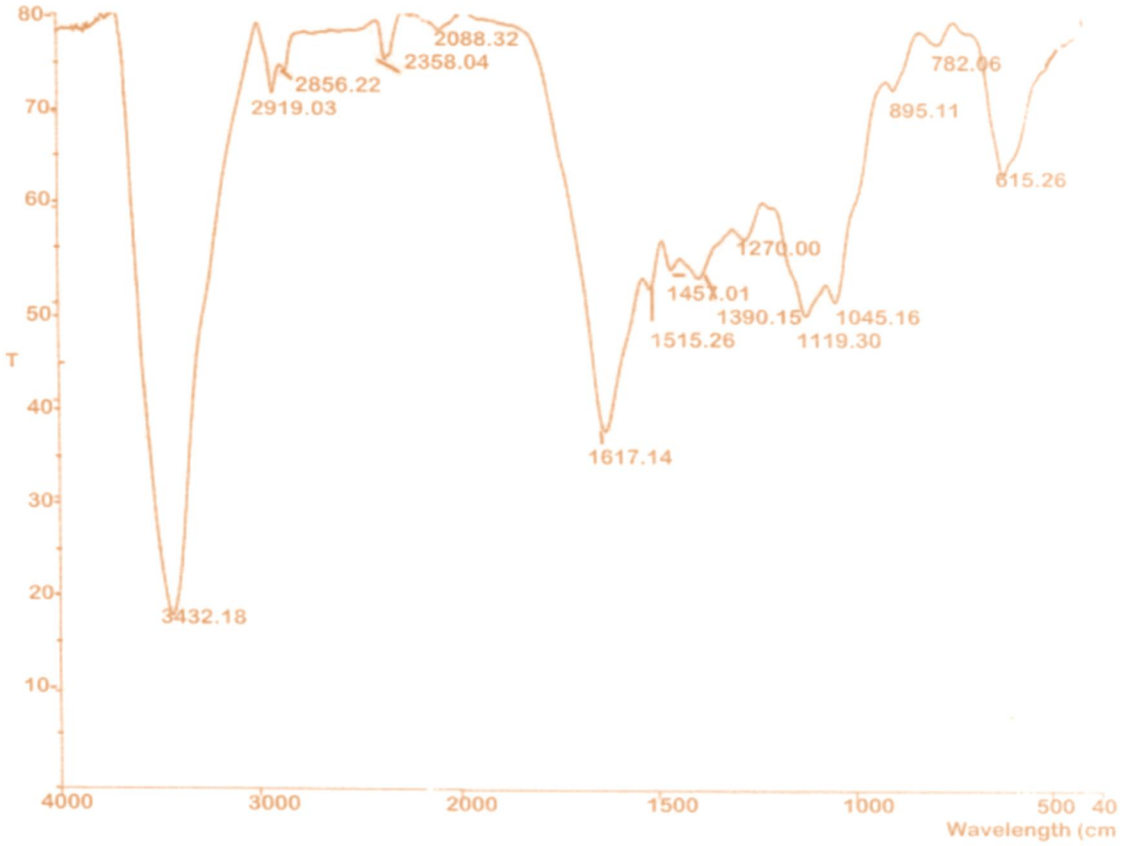

Figure 2. FT-IR of the 1% sodium hydroxide extract

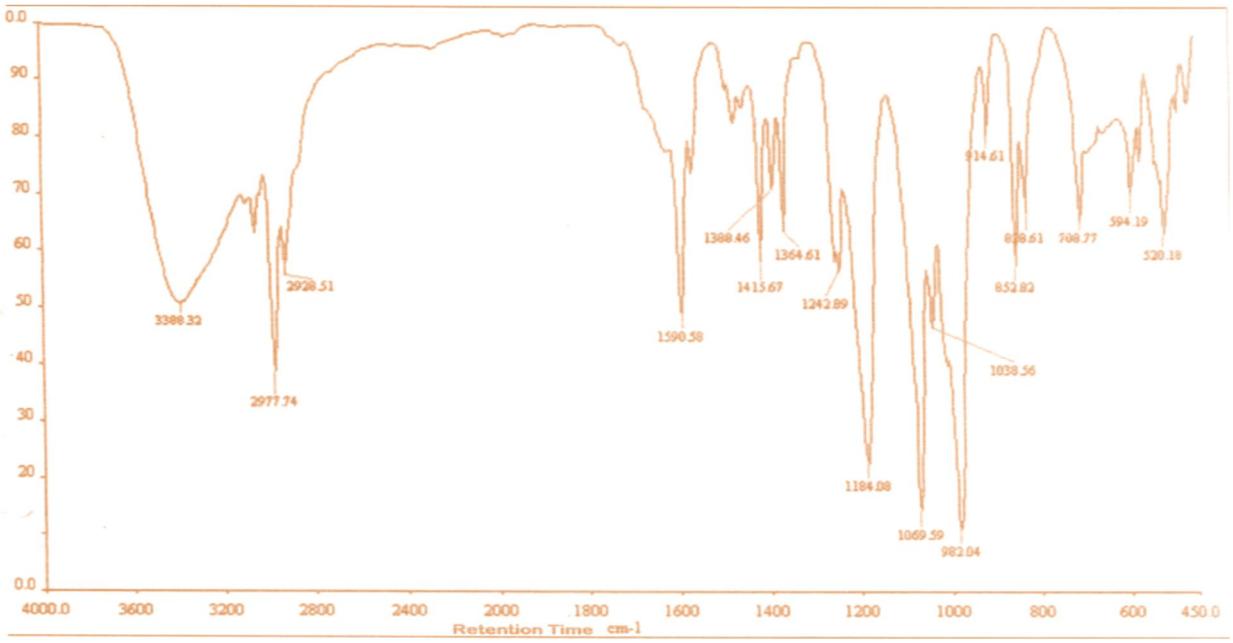

Figure 3. FT-IR of the methanolic dye extract

The results of the infrared spectral analysis of the various dye extracts from the dried sunflower petal using water, methanol and 1% NaOH respectively as the extracting solvents (Figures 1, 2, & 3) revealed the presence of various peaks ranging from C-H stretching, O-H, C=O, N-H and other several bands. The aqueous dye extract under investigation showed the presence of C-H stretching at wavenumber of 2770 cm^{-1} and amide group with N-H bending at 1564 cm^{-1}.

The presence of chromophore and auxochrome in each of the extracts reflected in the shade of colours observed. Chromophores are represented as nitrogen, carbon and oxygen which usually have single or double bonds which are primarily essential for colour formation. The parent compounds containing them are termed chromogen. The auxochromes are polar groups that greatly increase the colour yielding power of chromophores [22] but when present alone will fail to produce that colour hence they are called colour helpers.

The following peaks were observed in the aqueous extract; 3305 cm^{-1} observed is assignable to H-bonded and O-H stretching vibration, 2770 cm^{-1} related to C-H stretching while 1460 cm^{-1} assigned for O-H bending was possibly from alcoholic group. The peaks observed at 1725 cm^{-1} or 1607 cm^{-1} could be assigned to C=O bending to stretch vibration The methanolic extract revealed a wavelength of 1364.61 cm^{-1} of bending vibration of benzene derivatives while the C=C-C functional group is an indication of the presence of aromatic rings. The NaOH extract revealed the presence of N-H_4^+ functional group in it while the peak value at 1617.14 cm^{-1} possibly represents C=C stretching vibration due to aromatic ring deformation. The peaks at 3432.18 cm^{-1} and 2919.03 cm^{-1} are assignable to O-H stretching vibration.

The O-H group that was found to be present uniformly in all the extracts has the ability to form hydrogen bond which is an indication of higher potential towards inhibitory activity against microorganisms [17]. Some of the peaks observed for the aqueous and methanolic extracts of *H. annuus* petals were similar to those observed for the yellow dye of *Carthamus tinctorius* by Shin and Dong [23]. The IR spectra obtained from this work could be compared with the standard dye databases from literature [14,16,24] or any available literature that contain IR spectra of several classes of dyes with known chemical structures and composition to accurately placed the extracted dyes from the different solvents to enhance their uses.

4. Conclusions

The results of this research work showed that natural dye of different shades of colours can be extracted successfully from the petal of sunflower using different solvents which could serve as an alternative to the synthetic colourants. The work also revealed that the dye extracts have different useful functional groups.

Acknowledgements

Authors gratefully acknowledge the Management of Osun State Polytechnic, Iree, Nigeria for the free use of laboratory facilities.

Funding

No financial support received for this research work.

References

[1] Rauf, M.A., Soliman, A.A., Khattab, M., 2008. Solvent effect on the spectra properties of neutral red. Chem. Central J. 2, 19.

[2] Adeoye, M.D., Abdulsalami, I.O., Oyeleke, G.O., Alabi, K.A., 2019. Theoretical studies of solvent effects on the electronic properties of 1, 3-Bis [(Furan-2yl) Methylene] Urea and Thiourea", J. Phys & Theor. Chem. of Islamic Azad University of Iran. 15(3, 4), 115-125.

[3] Ondarroa, M., Sharma, S.K., Quinn, P.J., 1986. Solvation properties of Ubiquinone-10 in solvents of different polarity. Biosci. Rep. 6(9), 783-796.

[4] Homocianu, M., Airinei, A., Dorohoi, D.O., 2010. Solvent effects on the electronic absorption and fluorescence spectra. J. Adv. Res. Phys. 2(1), 011105.

[5] Targema, M., Obi-Egbedi, N.O., Adeoye, M.D., 2013. Molecular structure and solvent effects on the dipole moments and polarizabilities of some aniline derivatives. Comput. & Theor. Chem. 1012, 47-53.

[6] Khan, M.F., Rashid, R.B., Rahman, M.M., Al Faruk, M., Rahman, M.M., Rashid, M.A., 2017. Effects of solvent polarity on solvation free energy, dipole moment, polarizability, hyperpolarizability and molecular reactivity of Aspirin. Int. J. Pharm. Sci. 9, 217-221.

[7] Saravanan, P., Chandramohan, G., Saivaraj, S., Deepa, D., 2013. Extraction and application of eco-friendly natural dye obtained from barks of Odina wodier L on cotton fabric. Scholar Res. Lib. 3, 80-85.

[8] Nurunnesa, Hossain, M.A., Rahman, M.M., 2018. Extraction of natural dye collected from the outer skin of onion and it's applications on skin fabric. Global J. Res. Eng. 18(3 Ver. 1), 1-6.

[9] Samanta, A.K., Konar, A., 2011. Dyeing of textiles with natural dyes. In: Kumbasar, E.A., Ed., Natural

Dyes, Intech Open, London. 29-56.
[10] Uddin, M.D., Razzaq, M.A., Quadery, A.H., Chowdhury, M.J., Al-Mizan, Raiman, M.M., Ahmad, F., 2017. Extraction of dye from natural source (LAC) and its application on leather. Amer. Sci. Res. J. Eng., Technol. & Sci. 34(1), 1-7.
[11] Saravanan, P., Chandramohan, G., Mariajacyrani, J., Saivaraj, S., 2015. Effect of chitosan and mordants on the dyeability of cotton fabrics with a natural dye from the barks of Odina wodier Roxb. J. Indian Chem. Soc. 92(6), 1007-1007.
[12] Saravanan, P., 2013. A study on the extraction and application of eco-friendly natural dye from barks of Odina wodier on silk fabric. Int. J. Curr Res. 5(5), 1070-1073.
[13] Saravanan, P., Chandramohan, G., Saivaraj, S., 2012. A study on the eco-friendly natural dye extracted from flowers of Lanntana camara L. on silk and wool fabrics. Asian J. Res. Chem. 5(3), 418-421.
[14] Nnorom, O.O., Onuegbu, G.C., 2019. Authentication of Rothmannia whitfieldii dye extract with FTIR Spectroscopy. J. Tex. Sci. & Techn. 5, 38-47.
[15] Olajire, A.A., 2011. Principles and applications of spectroscopic techniques. Ibadan, Ogfat Publications.
[16] Yuen, C.W.M, Ku, S.K.A., Choi, P.S.R., Kan,C.W., Tsang, S.Y., 2005. Determining functional groups of commercially available ink-jet printing reactive dyes using infrared spectroscopy. Res. J. Tex. & Apparel. 9(2), 26-38.
[17] Ashokkumar, R., Ramaswamy, M., 2014. Phytochemical screening by FTIR spectroscopic analysis of leaf extracts of selected Indian medicinal plants. Int. J. Cur. Microbiol. & Appl Sci. 3(1), 395-406.
[18] Kakeru, P.G., Keriko, G.J.M. Kenji, A.N., 2008. Direct detection of triterpenoid saponins in medicinal plants. Afr. J. Trad., Complem. & Altern. Med. 5(1), 56-60.
[19] Charushila, D., Swaroopa, P., 2016. FT-IR spectroscopic screening of phytochemicals of two medicinally important species of Solanum used in preparation of Dashmula formulation. Int. J. Pharm. Sci. & Res. 36(2), 112-120.
[20] Pakkirisamy, M., Kalakandan, S.K., Ravichandran, K., 2017. Phytochemical screening, GC-MS, and FT-IR analysis of methanolic extract of Curcumia caesia Roxb (Black turmeric). Pharmacog. J. 9(6), 952-956.
[21] Sayani, C., 2019. Fourier transform infrared (Ft-ir) spectroscopic analysis of Nictianaplum baginifolia (Solanaceae). J. Med. Plant Studies. 7(1), 82-85.
[22] Popoola, A.V., 2015. Chemistry of colours in dyes and pigments. (Allen, TX US & Lagos, Nigeria). Wits Publishing Ltd. 1-40.
[23] Shin, Y., Yoo, D., 2012. Storage stability and colour reproducibility of yellow and red dyes extracted from Carthamus tinotorius L. J. Tex. Colora. & Finish. 24(3), 155-172.
[24] Coates, J., 2000. Interpretation of infrared spectra. A practical approach. In: Meyers, R.A., Ed., Encyclopedia of analytical chemistry, John Wiley and Sons Ltd., Chichester. 1-23.

BILINGUAL PUBLISHING CO.
Pioneer of Global Academics Since 1984

Organic Polymer Material Research
https://ojs.bilpublishing.com/index.php/opmr

REVIEW

Research on Relationships between the Pigment of Dunhuang Mogao Grottoes Frescoes and Ecological Microorganism

Yiran Zhao[1*] Yu Guo[2]

1. University College Dublin, Beijing, 100036, China
2. Central South University, Shanghai, 410000, China

ARTICLE INFO

Article history
Received: 29 November 2021
Accepted: 24 December 2021
Published: 31 December 2021

Keywords:
Mural paint
Color change
Microorganisms
Protective measures

ABSTRACT

Dunhuang Mogao Grottoes is one of the largest art treasures in the world. She has a large number of murals, sculptures, beautiful and vivid; There are precious Buddhist scriptures, documents, noble and elegant. Spanning more than 1,600 years, the Mogao Grottoes show the world the extensive and profound Chinese culture with a long history. But over time, the murals in the Mogao Grottoes have also changed a lot. Thousands of years of wind and rain erosion, changes in the surrounding environment, and the influence of various biological communities have caused serious color changes and fading of murals in Mogao Grottoes. To slow down the color change of Dunhuang frescoes, protection measures should be taken from the perspective of ecological microorganisms. At present, Cladosporium, Planococcus, Phoma, Chaetomium, and other strains have caused serious discoloration or discoloration of murals to a certain extent. This paper studies the main color of Dunhuang frescoes, red, and summarizes the discoloration factors and mechanism of red lead. On this level, one should try to keep the murals and control the indoor temperature. Humidity, people, and other factors slow the fading of the murals. But these are often insufficient to protect the integrity of the murals, so we have conducted a review of the literature to provide an updated overview of the available evidence on the subject.

1. Introduction

Red lead is widely used, not only in Dunhuang murals but also in any ancient painting elements. Red lead is even used in murals all over the world, both at home and abroad. However, as time goes by, red lead in murals will gradually change from red to black or fade. The main factors affecting the discoloration of red lead are light, humidity, microorganism, and part of salt solution. Red lead is the main part of Dunhuang murals. The color change and fading of red have a great influence on the murals [2].

1.1 Microorganisms Cause the Discoloration

As a strong oxidant oxidation color pigment, Pb_3O_4 is

**Corresponding Author:*
Yiran Zhao,
University College Dublin, Beijing, 100036, China;
Email: 2812362617@qq.com

DOI: https://doi.org/10.30564/opmr.v3i2.4158

also known as red lead, red lead has strong stability, high corrosion, rust resistance, and high heat resistance, but not acid resistance, but because of the presence of high lead ions in the red lead, can be oxidized by a strong oxidant. This confirms that most of the black material on the mural is PbO_2 [3,6]. It is found that the microbial cause of the discoloration of Dunhuang frescoes is the oxidation of red lead into PbO_4 by Flavobacterium. Many people have also mentioned the existence of a large amount of oxalate in murals. In the disease investigation of Dunhuang murals mentioned in literature [11], it was found that copper oxalate was often present in the red lead and black paintings. The origin of oxalate is derived from microbial metabolites, which are often found in hydrogen peroxide. It is mentioned that the humid environment in the cave provides necessary conditions for microbial metabolic activities, organic matter in the coating layer provides sufficient nutrients for microorganisms, and darkness (or light) promotes the growth of microorganisms. As mentioned above, hydrogen peroxide exists in the metabolites of microorganisms, so it can be seen that the discoloration of red lead is partly due to hydrogen peroxide in the metabolites of Falfa bacteria, which leads to oxidation of red lead from red to black, and finally exists in the form of lead dioxide in the fresco [5].

1.2 The Salt Solution of Carbon Dioxide Causes the Discoloration

At the same time, carbon dioxide and soluble salt also have some influence on the discoloration of red lead.

According to the sampling 98 wats [9] soluble salt rock is mainly sulfate and chloride salt and contains a small amount of HCO^{3-} and NO^{3-}, and because the Mogao grottoes as an important cultural site, tourism, hotels increased, leading to rising carbon dioxide levels in the caves, thus rising humidity, these will make red lead is oxidation, discoloration.

$Pb_3O_4+4HNO_3=PbO_2+2Pb(NO_3)_2+2H_2O$ [5]

Wang Julin et al.[5] proposed that in the environment of carbon dioxide, the discoloration of red lead is the most serious in sulfate solution, while the discoloration degree is less in a mixed salt solution. However, no matter the presence of carbon dioxide or not, the red lead will change from lead to $PbCO_3$ and PbO_2 after being soaked by water.

1.3 Chlorine Salts Cause Color Changes

Shimadzu, Yoshiko et al. once experimented, spraying artificial seawater on wooden objects coated with lead, and the content of salt mineral substance was 2.7wt%. After some time, they found that red lead on these wooden objects changed color, which was inferred to be related to the crystalline salt in the seawater [12]. The main components of crystalline salt are NaCl and Na_2SO_4, mainly in the form of Na^+, Cl^-, and SO_4^{2-}. Because red lead is an oxidation color change, it is speculated that Cl^- and $NaSO_4^{2-}$ may play an oxidation role. Since it is artificial seawater, it is mainly considered that the strong oxidation of Cl^- leads to the color change of red lead. In the experiment by Sister Daniilia and Elpida Minopoulou, they used Optical microscopy, FTIR spectroscopy and Scanning electron microscopy (SEM/EDS) was used to detect the elements in the mural, especially in the red part of the mural that has become gray. The partial alteration was found through Scanning electron microscopy (SEM/EDS), and cinnabar mixed with calcium carbonate. At the same time, the presence and high abundance of Cl^- were detected [1], which also explained the main reason for the color change of much red lead in the seashore.

Figure 1. Unoxidized red lead

Source: Baidu pictures

Figure 2. PbO_2

Source: Baidu pictures

2. Microorganisms in the Air where Dunhuang Frescoes are Located

2.1 Method

Factors affecting microbial concentration in air of Dunhuang with control variables. According to the Study

of Air Fungal Ecology in Dunhuang Mogao Grottoes, the main factors affecting the concentration of air fungi in Dunhuang Mogao Grottoes include temperature, relative humidity, and human activities.

Sample 1.

Vacuum sterile glasses were used to sample the air in the mogao grottoes four times. After sampling, sealed glasses were numbered 1,2,3,4, and the change of fungal concentration in the glasses was monitored.

(1) Place no. 1 cup in normal air to monitor its fungal concentration

(2) The no.2 cup was properly heated, other conditions were kept the same as the no.1 cup, and the change of fungal concentration in the cup was monitored.

(3) Change the relative humidity of no. 3 cup, keep other conditions the same as that of No. 1 cup and monitor the change of fungal concentration in the cup.

(4) Mix the air people have breathed into cup no. 4, keep other conditions the same as cup No. 1, and monitor the change of fungal concentration in the cup.

2.2 The Experimental Results

(1) Compared with no. 1 cup, with the increase of temperature, the fungal concentration in No. 2 cup increased in a certain range

(2) Compared with No. 1 cup, the fungal concentration in No. 3 cup increased when the relative humidity was higher, and the fungal concentration in No. 3 cup was lower when the relative humidity was lower

(3) Compared with cup 1, the concentration of fungi was higher in cup 4 mixed with air that humans had breathed

2.3 The Experimental Conclusion

(1) The concentration of fungi in the air of Dunhuang Mogao Grottoes is affected by temperature. Within a certain range, the higher the temperature is, the higher the concentration of fungi will accelerate the fading of mogao grottoes frescoes. The increase of temperature led to the increase of fungal metabolic rate, the increase of metabolites produced by fungi, and the acceleration of the redox process. If the murals are in this environment, red lead in the murals will cause a serious color change.

(2) The concentration of fungi in the air in Dunhuang Mogao Grottoes was affected by relative humidity. The higher the relative humidity was, the easier the fungi were to reproduce, and the easier the mogao grottoes murals were to fade. The relative humidity is low, the concentration of fungi in the air is low, and the mural is not easy to fade. Because the increase of humidity will lead to the increase of water molecules, and in a high humidity environment, any metal substance will be affected by the action of water molecules and oxygen in the air, to carry out redox reactions and lead to the change of lead color.

(3) The concentration of fungi in the air of Dunhuang Mogao Grottoes is affected by human activities. Human activities change the composition of gases in the air. The more people there are, the faster the growth and reproduction of fungi will be, and then the fading of murals will be accelerated. Bacteria and fungi are everywhere in the environment, especially the bacteria carried by the human body, and their metabolites will cause irreversible color changes to the murals.

(4) In fact, it is not difficult to see that the dry and cold environment is conducive to the preservation of the murals, to reduce the conditions and factors leading to the redox reaction of red lead in the murals. To protect the mural. The mogao Grottoes also use this method to protect murals under the condition of controlling temperature, humidity, and passenger flow. Although we say that we need to reduce the mural color change caused by fungi and other influencing factors in a dry environment, too dry conditions will also cause cracking, falling off and other effects on the mural, so at present, we are applicable to the way of constant temperature and humidity control

According to "Research on the Prevention and Control of Fungal Diseases in Dunhuang Murals", [7] inhibitors such as mercury chloride and butyl tin chloride have significant antibacterial effects, which can also affect the concentration of fungi in the air in Mogao Caves, so they are effective.

3. Protection of Dunhuang Frescoes

In fact, during the Sino-Japanese War of 1894-1895, people had already carried out the protection of the Murals in Mogao Grottoes. However, due to the poor conditions, harsh environment, and underdeveloped science and technology at that time, people could only reduce the passenger flow and limit the phenomenon of cultural relics being stolen again in the grottoes. As time went on and technology developed, people began to use existing technology to reinforce and repair the caves. At present, the protection of caves is mainly carried out from three aspects: geology, ecological environment, and human influence. For example, people use baffles and cement floors to prevent the wear of wind sand and strong ultraviolet radiation. Even though dust and sundries in the caves are cleaned, weather stations are established to monitor the harsh environment in the area in real time,

and rules and regulations are used to protect the caves and murals [4].

3.1 Protection of Murals in Caves

According to the experimental results, high temperature, high humidity and more people flow will increase the concentration of fungi in the air to a certain extent, and then accelerate the color change and fading of Dunhuang murals. Therefore, relevant departments in Dunhuang should take measures to control the temperature, relative humidity, and the number of tourists in the Mogao Grottoes, strengthen the behavior management of touristsreal-tim and avoid uncivilized behaviors that further harm the murals.

Inhibitors such as mercury chloride and tributyltin chloride were used to inhibit the growth and reproduction of bacterial microorganisms. Generally, bacteria and viruses are made up of proteins. Mercury chloride is a heavy metal salt, and mercury ions are heavy metal ions. Protein molecules can combine with positively charged metal ions to form protein salts, and irreversible precipitation of proteins occurs (heavy metal ions precipitate proteins). Butyltin chloride can be effectively anticorrosive, and protect murals from corrosion [8].

Through the correlation analysis of information decoding and digital construction, the digital integration technology is applied to integrate multi-dimensional architectural information into graphic image recombination processing to realize the digital regeneration of Dunhuang mural architecture. Explore the technical methods, realization approach,hes and application values of digital reproduction and reconstruction, and expand the methods and paradigms of preservation and inheritance of mural architecture in the new context [10].

Dunhuang locals should pay attention to ecological construction, establish a good ecological environment, to improve the air inside the Mogao Grottoes, and then reduce the concentration of fungi and microorganisms, to slow down the fading effect of the frescoes.

The restoration of Dunhuang murals should be increased. The faded murals should be restored to their original colors and protected.

3.2 The Protection of the Overall Environment for the Murals

The number of daily visitors should be controlled to reduce the CO_2 concentration and humidity in the cave at the same time. Establish a natural ecological protection area [13]. The geographical position of Dunhuang is easily affected by wind and sand.

4. Conclusions

According to literature review and simulation experiments, hydrogen peroxide, carbon dioxide, sulfate, nitrate and chloride are the main causes of lead discoloration in our daily life. Based on these mechanisms, these methods have also been used for heritage conservation.

The natural color red lead in Dunhuang frescoes is a kind of chemical change. Despite the influence of microorganisms, the discoloration mechanism caused by red lead and microorganisms can be attributed to REDOX reaction, which can also be in ecology and microbial metabolism, and finally lead to color change or microbial metabolites.

The world is big, the development of science and is constantly, technology in the unceasing evolution, mural color changes in the city, I don't know what exists in China, more exist all over the world, the color of the murals are different, this article briefly summarizes the main color change and response mechanism of red lead, now people are constantly trying to protect cultural relics, it is not only a symbol of culture and history of each country, It is also the cultural heritage of the whole human world, which deserves protection. Although it cannot show the glory of the past, it is worth people to protect the murals and cultural relics of the present and future, so that they can be handed down forever.

Acknowledgment

This is the end of the article. Here, we sincerely express our gratitude to the teachers who taught us the word. It is you who let us know the beauty, the long history, and the splendid culture of Dunhuang. I would also like to thank the members of other groups. Your discussions and suggestions have given us a lot of help. We are also grateful to the authors of the paper who provided us with experimental data, information, etc., which made this paper possible. Thank you again

References

[1] Daniela, S., Minopoulou, E., 2009. A study of smalt and red lead discoloration in Antiphonitis wall paintings in Cyprus. Applied Physics A. 96(3), 701-711.

[2] Gong, M.T., Xin, X.H., Han, F., et al., 2009. Study on the color change of lead. Culture and Museum. 6, 8.

[3] Hideki, N., Changlong, K., 1991. Reactivity of lead lead. Huafeng Information. 2, 15. (in Chinese)

[4] Jinshi, F., June 1997. Fifty years of protection of the

Dunhuang Grottoes. In Conservation of Ancient Sites on the Silk Road: Proceedings of an International Conference on the Conservation of Grotto Sites, ed. Neville Agnew. pp.12-22.

[5] Wang, J.L., 2014. Corrosion science and protection technology. 02, 159-162.

[6] Wang, L.W., 2008. Western archaeology. 00, 293-298.

[7] Zhang, M.L., 2012. Study on the control of mold diseases in Dunhuang murals. Lanzhou Jiaotong University.

[8] Ma, Z.Y., Wu, X.M., 1981. Antibacterial activity of dichloroethylsalicylamides. Chemical World. 10, 9-10.

[9] Guo, Q.L., 2009. Journal of rock mechanics and Engineering. S2, 3769-3775.

[10] Li, Q.Q., Chao, Zh., Chao, W.B., Chao, J., 2019. Digital protection of cultural Heritage. Southeast Culture. S01, 4.

[11] Rachael D Wakefield, Melanie S Jones : Quat J Eng Geol. 1998. pp. 30l.

[12] Shimadzu, Y., Morii, M., Kawanobe, W., 2002. A study of discolouration of the red lead coating (ni-nuri) on historical wooden buildings in a seafront environment [Original title and text in Japanese]. Science for conservation. 41, 113-120.

[13] Lv, X.Y., 2019. On the construction of Dunhuang Cultural and Ecological Reserve. Yanshan University.

BILINGUAL PUBLISHING CO.
Pioneer of Global Academics Since 1984

Organic Polymer Material Research
https://ojs.bilpublishing.com/index.php/opmr

ARTICLE

Study of Hydrophilic Properties of Polysaccharides

Michael Ioelovich*

Designer Energy, Rehovot, 7670504, Israel

ARTICLE INFO

Article history
Received: 08 December 2020
Accepted: 27 December 2021
Published Online: 30 December 2021

Keywords:
Polysaccharides
Amorphous domains
Structure
Specific surface area
Sorption of water vapor
Enthalpy of wetting
Hydrophilicity index
Calculations

ABSTRACT

In this research, the structural characteristics, specific surface area, sorption of water vapor, and wetting enthalpy of various polysaccharides (cellulose, hemicelluloses, starch, pectin, chitin, and chitosan) have been studied. It was confirmed that crystallites are inaccessible for water, and therefore water molecules can interact only with polar groups in noncrystalline (amorphous) domains of biopolymers. The isotherms of water vapor sorption for various polysaccharides had sigmoid shapes, which can be explained by the absorption of water molecules in heterogeneous amorphous domains having clusters with different packing densities. The method of contributions of polar groups to sorption of water molecules was used, which allowed to derivate a simple calculating equation to describe the shape of sorption isotherms. The wetting of biopolymers with water was accompanied by a high exothermic thermal effect, in direct proportion to the amorphicity degree. The sorption values and wetting enthalpies of amorphous domains of biopolymers were calculated, which allowed to find the hydrophilicity index and compare the hydrophilicity of the various polysaccharides.

1. Introduction

Polysaccharides are an important class of biopolymers synthesized in living organisms such as plants, animals, and microorganisms, from which these biopolymers can be extracted [1-3]. The polysaccharides can be amorphous or semicrystalline, and composed of the same (homo-polysaccharides) or different (hetero-polysaccharides) monomeric units; in addition, hydroxyl groups of these units can be substituted by other groups. Polysaccharides may comprise residues of various monosaccharides such as glucose, fructose, mannose, galactose, xylose, etc. Depending on whether the monomeric unit contains 5 or 6 carbon atoms, polysaccharides are classified also into C5- and C6-polysaccharides.

Known types of polysaccharides are cellulose, starch, mannan, xylan, pectin, chitin, chitosan, and others. The most widespread polysaccharide in nature is cellulose [4]. Cellulose is a linear, stereoregular, high molecular, and semicrystalline biopolymer composed of repeating D-anhydroglucose units (AGU) linked by β-1,4-glycosidic bonds. This polysaccharide occurs in all terrestrial plants

**Corresponding Author:*
Michael Ioelovich,
Designer Energy, Rehovot, 7670504, Israel;
Email: ioelovichm@gmail.com

DOI: https://doi.org/10.30564/opmr.v3i2.4181

and many algae; in addition, cellulose is found in shells of certain marine creatures, and this biopolymer is synthesized by some microorganisms, e.g. *Gluconacetobacter xylinus*.

Mannan and xylan, also called hemicelluloses, are found in all terrestrial plants [5]. They are low crystalline and low molecular biopolymers. Mannan is a polysaccharide containing mannose units linked by β-1,4-bonds. In addition to mannose, mannan may contain residues of glucose and galactose. Xylan consists of xylose units connected by β-1,4-bonds. This polysaccharide usually also contains 9%-10% residues of 4-O-methylglucuronic acid.

Starch is a complex polysaccharide consisting of two main components amylose and amylopectin [6]. Amylose is a linear carbohydrate, glucose units of which are connected by α-1,4-glycosidic bonds. Amylopectin is a branched carbohydrate, containing α-1,4-glycosidic bonds in linear segments and α-1,6-glycosidic bonds in branches. Due to such structure, low crystallinity, and low degree of polymerization (DP), starch is soluble in hot water and turns into a gel when cooled.

The carboxylated polysaccharide, pectin, and the nitrogenized polysaccharides, chitin, and chitosan are also well known. Linear chains of pectin contain units of D-galacturonic acid joined by α-1,4-bonds. Pectin is an amorphous, low-molecular biopolymer that is soluble in hot water to form a gel.

Chitin is the most widespread nitrogen-containing polysaccharide in nature, which is present in exoskeletons and shells of some aquatic animals and insects, as well as in the cell walls of some fungi and microorganisms [7]. Chitin is regarded as a nitrogenized derivative of cellulose, where the hydroxyl group at C2 atoms in each AGU is replaced with an acetylamino group. Macromolecules of this natural polymer contain up to 10,000-15,000 units of 1,4-β-N-acetylglucosamine. Similar to cellulose, chitin is a linear semicrystalline biopolymer. Chitosan is a nitrogenized polysaccharide containing amino groups in glucosamine units of macromolecules. This biopolymer is produced mainly by deacetylation of chitin with hot sodium hydroxide. Like chitin, chitosan is a linear semicrystalline biopolymer. A distinctive feature of chitosan is easy dissolution in dilute acids and subsequent regeneration from the solutions after neutralization.

Despite the difference in structure and origin, almost all polysaccharides have such specific features as an affinity for water, i.e. they are hydrophilic polymers. To study hydrophilicity, various methods can be used, such as measuring the contact angle of a water drop on the surface, the degree of swelling, sorption of water vapor, enthalpy of wetting, and some others. However, to measure the contact angle, the surface of the sample must be flat, homogeneous, free of roughness and pores [8,9], which in many cases is difficult to implement in practice. The measurement of the degree of swelling is not standardized and depends on the conditions of sample preparation, its external structure (powder, fiber, sheet, or film), and the method of removing the water excess, etc. The most accurate and reproducible methods for studying hydrophilicity are considered the sorption of water vapor and the enthalpy of wetting.

When studying the sorption isotherms of water vapor (WV) for cellulose and other polysaccharides it was found that these isotherms are S-shaped, i.e. they are type II. This type of isotherm is usually explained by multilayer surface adsorption of water molecules, which is described by BET, GAB, or some other adsorption equations [10-12]. The analysis of the GAB equation showed that the common tree-parametric GAB equation describes the sorption isotherms with low accuracy, especially at increased relative vapor pressures or water vapor activities [13]. If the number of parameters of the GAB equation increases, the accuracy improves. However, in this case, the parameter of monolayer capacity becomes a variable value, and the calculations of the specific surface area of biopolymers become unreliable.

Park's sorption model provides the use of the Langmuir equation of monolayer surface adsorption at the initial stage, Henry's equation of WV dissolution in biopolymer at the middle stage, and a power-law equation describing the clustering of water molecules at the last stage of sorption [14,15].

However, the problem is that in reality the equations of monolayer and multilayer surface adsorption of WV are unsuitable for calculating the structural parameters of polar hydrophilic biopolymers since the sorption mechanism is not the adsorption of sorbate molecules on the surface of pores, but the absorption of polar water molecules inside the noncrystalline (amorphous) domains of the polar polymers [16-18]. In this case, to calculate the isotherms of WV for biopolymers, it is necessary to use the thermodynamic equation [19] or other equations describing the absorption process such as Henry, Hailwood Horrobin, etc. [15,16,20].

Discussing Park's model it should be noted that the presence of a linear dissolution process of WV in polysaccharides following Henry's law is unlikely since this law is observed only for ideal solutions, to which the polysaccharide-water system does not belong. In addition, the clustering of water molecules in hydrophilic biopolymers at the last stage of sorption was not found. Moreover, to describe each isotherm, Park's model

requires the determination of at least five parameters [15]. If it is necessary to describe the isotherm of WV for another biopolymer sample, then the new five parameters must be recalculated. Thus, Park's model is mathematically adapted to the experimental isotherm without proof of the sorption mechanism.

The Hailwood and Horrobin model postulated the dissolution of VW in the internal structure of biopolymer during the sorption process with the formation of monohydrates and polyhydrates [20]. However, this hypothesis is doubtful since polysaccharides cannot form chemical compounds with water such as monohydrates. It has also not been proven that the formation of polyhydrates should actually lead to a hyperbolic increase in the amount of sorbed water. The parameters of Hailwood and Horrobin's equation are selected in such a way as to achieve the best agreement with the experimental isotherm. This assists to adapt the model to the experiment but does not provide arguments about the real sorption mechanism.

Many arguments are indicating the absorption mechanism of the interaction of water molecules with polysaccharides. For example, it is known that cellulose and other carbohydrates in the dry state are low-porous sorbents, whose specific surface measured by the sorption of inert gases and vapors is several square meters per gram [21,22]. In this case, the value of surface adsorption should be very low and cannot exceed one percent. However, in reality, the amount of WV sorbed by biopolymers reaches several tens and even several hundred percent.

If such polysaccharide as natural cellulose is mercerized or dissolved in a solvent and then regenerated from the solution, the specific surface area of the obtained samples decreases [19]. Despite this fact, the sorption capacity of the samples for WV after these treatments, on the contrary, increases sharply, which is caused by amorphization of the biopolymer and increase in the content of amorphous domains providing higher accessibility of polar water molecules to the internal structure of polar sorbent [23].

In addition, the process of WV sorption by polysaccharides is accompanied by such phenomena as a swelling, partial dissolving of water-soluble biopolymers, decrease of the glass transition temperature and even melting point, and recrystallization of amorphized biopolymers, etc. [24,25]; furthermore, when these polysaccharides are wetted, a significant amount of thermal energy is released [26]. All these phenomena are obvious evidence for the absorption of water molecules by biopolymers.

Taking into consideration the absorption mechanism, in this article, a comparative study of the hydrophilicity of various polysaccharides was carried out by measuring the sorption of WV and the enthalpy of wetting. Since the crystallinity strongly affects the sorption capacity, to compare the hydrophilicity of samples with different crystallinity, it is necessary to use hydrophilic characteristics of amorphous domains of semicrystalline biopolymers. After that, the relative hydrophilicity index of various polysaccharides was calculated.

2. Materials and Methods

2.1 Materials

The following cellulose samples were investigated:

- Fine powder of microcrystalline cellulose (MC) Avicel PH-301 of FMC BioPolymer Co.
- Sheets of pure chemical-grade cotton cellulose (CC) of Hercules Co.
- Sheets of bleached spruce Kraft pulp (KP) of Weyerhaeuser Co.
- Fibers of mercerized Kraft pulp (MP) prepared by treatment with 20% NaOH and following washing and drying
- Yarn of viscose fibers (VF) of Rayonier Inc.

Purified powders of chitin (CT) from crab shells (degree of acetylation DA=94%) and chitosan (CS) (degree of deacetylation DDA=85%), potato starch (ST), citrus pectin (PC), birch xylan (XL), and mannan (MN) from *Ceratonia silique*, were acquired from Sigma-Aldrich.

2.2 Wide-angle X-ray Scattering (WAXS)

Wide-angle X-ray scattering (WAXS) studies were carried out using diffractometer Rigaku Ultima Plus in the 2θ angle range from 5° to 80°. CuKα radiation had wavelength λ = 0.15418 nm. Collimation included a system consisting of vertical slits and Soller slits. The procedure of 0.02° step-by-step scanning was used to determine the exact position of the peaks. The weak peaks were identified by a step-by-step scanning method with the accumulation of impulses at each step. A few of the diffractograms of the same biopolymer sample were recorded to obtain more reliable results. The incoherent background was subtracted from diffractograms. Then profiles of the isolated peaks were improved using corrections on absorption, combined PL factor, and Rietveld refinement. The angular positions of the peaks were checked using a narrow line of NaF standard at 2θ of 38.83°. Overlapped peaks were separated using the least-squares program.

The degree of crystallinity (X) of the biopolymer samples was calculated by the following equation [27]:

$$X = \int Jc\, d\theta / \int Jo\, d\theta \quad (1)$$

where *Jc* and *Jo* are the corrected and normalized intensities of X-ray diffraction from crystalline domains only and whole polymer sample, respectively.

In addition, the amorphicity degree (Y) of the samples was calculated, as follows:

$$Y = 1 - X \quad (2)$$

2.3 Sorption of Vapors

The sorption experiments were carried out at 25 °C on a vacuum Mac-Ben apparatus having helical spring quartz scales. Sorbates were water and n-hexane. Before starting the experiments the samples were dried at 105 °C up to constant weight and additionally degassed under vacuum in the sorption device. Three of the same samples were tested to calculate an average sorption value and standard deviation that was in the range ± 0.002 g/g. The value of s_m (g/g) corresponding to the inflection point of the isotherms was found, after which the specific surface value (S_{sp}, m^2/g) was calculated, as follows.

In the case of n-hexane vapor: $S_{sp}(H) = 2087\ s_m$ (3)

In the case of water vapor: $S_{sp}(W) = 3516\ s_m$ (4)

2.4 Enthalpy of Wetting

The enthalpy of wetting of biopolymers ($\Delta_w H$) was studied at 25 °C by the method of precise microcalorimetry using a TAM III calorimeter [28]. The samples were preliminarily dried at 105 °C in a vacuum chamber to constant weight. Three of the same samples were tested to calculate an average enthalpy value and standard deviation that was in the range ± 0.02 J/g.

3. Results

3.1 WAXS Studies of Polysaccharides

The study of X-ray diffraction showed that such samples as CT, KP, MC, and CC had intensive and narrow crystalline peaks, which is a sign of the quite high crystallinity of these samples (see e.g. Figure 1, Table 1). Samples of CS, MP, and VF exhibited broader crystalline peaks of medium intensity indicating their medium crystallinity (see e.g. Figure 2, Table 1).

Samples of PC, ST and hemicelluloses were characterized by broad and low intensive diffraction, which indicates an amorphized low-crystalline structure (see e.g. Figure 2, Table 1).

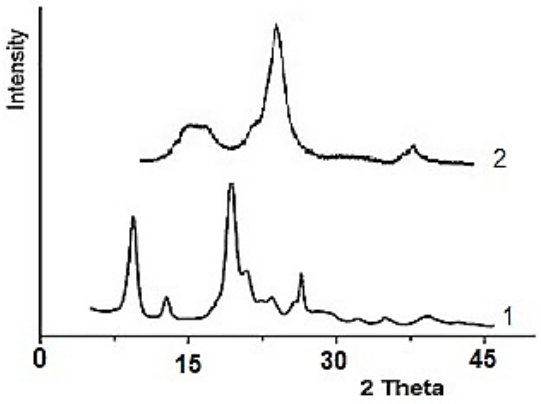

Figure 1. X-ray diffractograms for samples of CT (1) and KP (2)

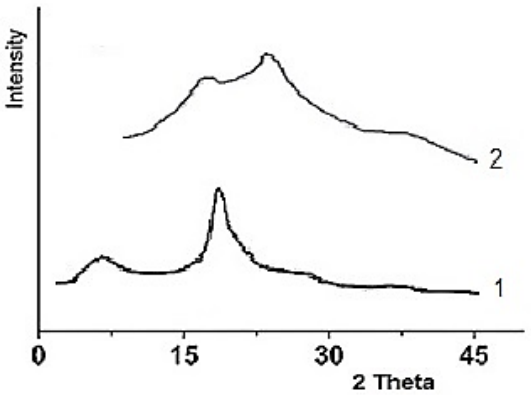

Figure 2. X-ray diffractograms for samples of CS (1) and PC (2)

3.2 Estimation of the Specific Surface Area of Polysaccharides

Sorption isotherms of n-hexane vapor for dry samples of MC and ST resemble isotherms of I (b) type, which have an initial steep part and then a gentle plateau (Figure 3). Therefore, to find s_m value the Langmuir equation was used

Despite higher crystallinity (X=0.75), the MC sample has a higher sorption value than the less crystalline ST sample (X=0.28). As a result, fine MC powder exhibits a higher specific surface area, S_{sp} (H), than starch grains (Table 1). Nevertheless, in all cases, the sorption value of n-hexane for biopolymer samples was relatively small, several milligrams per gram of dry sorbent. These features indicate the adsorption mechanism sorption of the inert sorbate molecules on the surface of low-porous biopolymers.

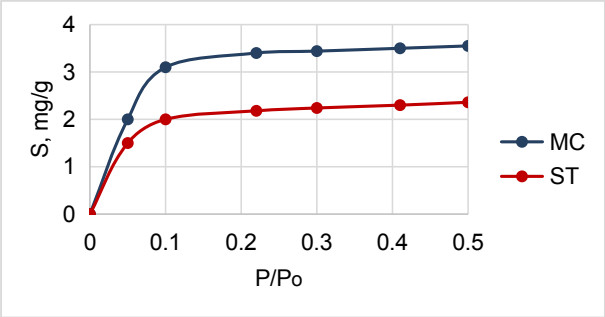

Figure 3. Sorption isotherms of n-hexane vapor for dry samples of MC and ST

Table 1. Specific surface area of polysaccharides measured by sorption of n-hexane [S_{sp} (H)], and water vapors [S_{sp} (W)]

Sample	X	Y	S_{sp}(H), m^2/g	S_{sp}(W), m^2/g
MC	0.75	0.25	7.1	84
CC	0.70	0.30	5.4	100
KP	0.64	0.36	6.3	122
MP	0.53	0.47	3.7	161
VF	0.36	0.64	3.0	200
ST	0.28	0.72	4.6	231
MN	0.26	0.74	6.5	242
XL	0.23	0.77	6.8	216
PC	0.20	0.80	6.0	232
CT	0.68	0.32	5.6	90
CS	0.46	0.54	5.2	180

In contrast to isotherms of type 1(b) characteristic for surface adsorption of inert sorbates (n-hexane), the sorption isotherms of water vapor for various samples had sigmoid shapes, and therefore they can be classified as type II (Figure 4). Isotherms of this type have an initial steep part, after which a gradual increase in sorption is observed, and finally, at high relative vapor pressures, a sharp increase in the sorption of WV occurs.

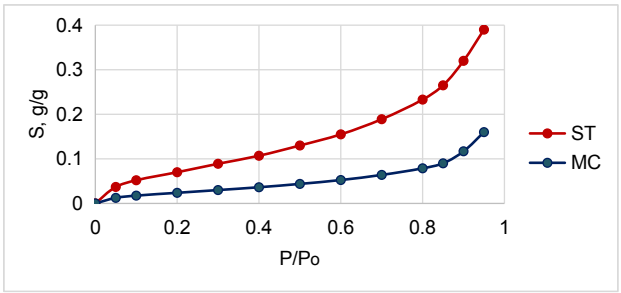

Figure 4. Sorption isotherms of water vapor for dry samples of MC and ST

In the coordinates of the BET equation, Z = φ/[(S (1-φ)] = F(φ), where φ =P/Po, the sorption isotherms of WV are generally nonlinear (Figure 5**).** To find s_m, the linear section of the BET isotherms was used in the φ range from 0.1 to 0.5. The specific surface area of biopolymers, S_{sp} (W), calculated from the BET sorption isotherms of WV is very high and reaches several hundred square meters per gram despite the fact that all studied samples in the dry state were low-porous (Table 1). Moreover, the study showed, there is no correlation between S_{sp} (W) and S_{sp} (H).

On the other hand, the linear correlation between the S_{sp} (W) value and the degree of amorphicity (Y) of samples is observed (Figure 6), which evidences the absorption mechanism sorption of WV in amorphous domains of various polysaccharides.

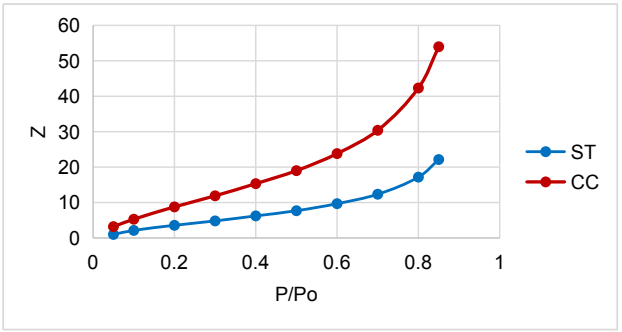

Figure 5. Sorption isotherms of water vapor by CC and ST in coordinates of BET equation

Thus, the S_{sp} (W) value does not characterize the porous structure of polysaccharides. In fact, the high value of S_{sp} (W) is an index of the accessibility of the internal structure of biopolymers to water vapor, which depends on the degree of amorphicity.

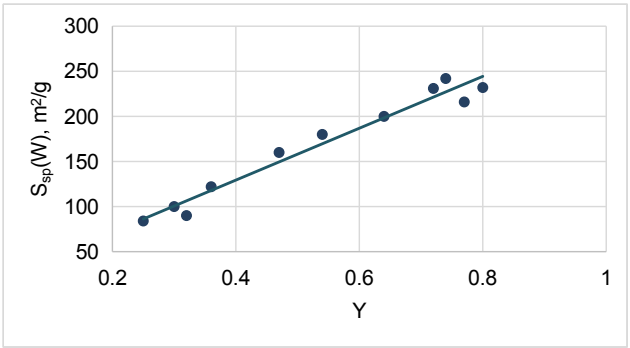

Figure 6. Linear correlation S_{sp} (W) = F(Y)

3.3 Water Sorption Ability of Functional Groups of Amorphous Biopolymers

To calculate the sorption isotherms of water vapor for amorphous polymers or amorphous domains of semicrystalline polymers at 25 °C, Van Krevelen proposed the contributions of various functional groups of polymers to the sorption of water molecules at several values of the relative vapor pressure, φ=P/Po [29]. It was found that only

polar groups are capable of attaching water molecules, while the contribution of non-polar aliphatic and aromatic groups to the sorption of WV was close to zero.

Calculations by the Van Krevelen method showed good agreement with the experiments. However, this method has also limitations. The first limitation is that the method of Van Krevelen allows one to reliably find only three to four points of the isotherm, which is insufficient for plotting the full isotherm. The second limitation is that the group contributions at high φ-values, 0.9 and 1, contain not only water molecules sorbed by functional groups, but also capillary condensed water, and therefore the contribution values need to be corrected.

To overcome the mentioned limitations of the Van Krevelen method, in this study an Equation (5) was derived for calculating the contributions of different polar functional groups to the sorption of WV over the all φ-range, from 0 to 1 (Table 2).

$$a_i = a_{o,i}\,(1 - K\,ln\varphi)^{-1} \quad (5)$$

where a_i and $a_{o,i}$ are contributions of polar groups to the sorption of WV at a certain φ and φ=1, respectively; moreover, a_i and $a_{o,i}$ have the dimension of mol H_2O per mol group, while K is coefficient.

Table 2. Parameters of Equation (5)

Polar functional groups	$a_{o,i}$ mol/mol	K
-OH, -NH_2, -NHCO-	1.44	2.6
-COOH	1.31	5
-C=O	0.30	6
-COO-	0.24	7
-O-	0.12	16

Parameters of Equation (5) allow calculation of the sorption values (A_a, mol/mol) of WV for amorphous domains (AD) of semicrystalline polysaccharide at various φ, knowing only the chemical formula of the repeating unit (RU) of this biopolymer including the type and content (n_i) of polar groups, as follows:

$$A_a = \sum n_i\, a_i \quad (6)$$

Moreover, the maximum amount of water molecules ($A_{o,a}$) absorbed by AD of polysaccharides at φ=1, can be also calculated (Table 3).

Table 3. Maximum amount of water ($A_{o,a}$, mol/mol) absorbed by AD of various polysaccharides

Polysaccharides	Formula of RU	MW	N_p	$A_{o,a}$
C5-Polysaccharides (C5P)	$C_5H_6O_2(OH)_2$	132	4	3.00
C6-Polysaccharides (C6P)	$C_6H_7O_2(OH)_3$	162	5	4.56
Amino C6P (CS)	$C_6H_7O_2(OH)_2NH_2$	161	5	4.56
Acetylamin of C6P (CT)	$C_6H_9O_4(NHCO)CH_3$	203	5	4.51
Carboxylated C6P (PC)	$C_5H_5O_2(OH)_2COOH$	176	5	4.30

MW is the molecular weight of RU of polysaccharide

N_p is a number of polar groups in repeat unit (RU) of AD

From the theoretical calculations, it follows that each repeating unit of AD of studied polysaccharides can attach from 3 (for C5P) to 5 (for C6P) water molecules, i.e. one polar group of the RU in AD sorbs a maximum of one water molecule. This conclusion is confirmed by the literature data [16,30]. Thus, monomolecular absorption of water molecules in AD of biopolymers is achieved only at a maximum vapor pressure φ=1. This behavior distinguishes the polar hydrophilic biopolymers from porous low- and non-polar polymers, in which water molecules cover the surface of pores with a monomolecular layer at a low vapor pressure, usually below φ = 0.3.

The sorption values (S_a) at various φ for AD of the polysaccharide expressed in gH_2O/g sorbent also can be calculated, as follows:

$$S_a\,(g/g) = A_a\,(mol/mol)\ x\ (18/MW) \quad (7)$$

As an example, it can calculate the sorption isotherm of WV for AD of C6-polysaccharide (C6P) having the formula of repeating unit $C_6H_7O_2(OH)_3$. Such a polysaccharide can be cellulose, starch, mannan, and other hexoses. The RU of such polysaccharides contains two ether groups and three hydroxyl groups. The results of calculations of the a_i-values for these polar groups using Equation (5) and sorption values (A_a) for AD of C6P at various φ are shown in Table 4.

Table 4. Calculated sorption values of WV for AD of C6P

φ	$2a_e$	$3a_h$	A_a	S_a
0	0	0	0	0
0.05	0.005	0.490	0.495	0.054
0.1	0.006	0.618	0.624	0.069
0.2	0.009	0.833	0.842	0.094
0.3	0.012	1.046	1.058	0.117
0.4	0.015	1.277	1.292	0.144
0.5	0.020	1.542	1.562	0.174
0.6	0.026	1.855	1.881	0.209
0.7	0.036	2.240	2.276	0.253
0.8	0.052	2.734	2.786	0.310
0.9	0.089	3.391	3.480	0.387
1.0	0.240	4.320	4.560	0.506

$2a_e$ is the contribution of two ether groups

$3a_h$ is the contribution of tree hydroxyls groups

A_a is the amount of WV absorbed by AD of C6P (mol/mol) at various φ

S_a is the amount of WV absorbed by AD of C6P, (g/g) at various φ

Based on the parameters of Equation (5) (Table 2), the isotherm of VW for AD of biopolymers, e.g. for C6P, can be drawn (Figure 7).

Further, this isotherm of VW for AD can be presented

in a linear form, as shown in Figure 8. Extrapolation of the linear plot $1/S_a = F(-\ln\varphi)$ to $\ln\varphi = 0$ gives the value 1/So,a, from which the maximum sorption value, So,a, can be found. In addition, the slope coefficient (k) of the plot can be also determined. As a result, the following equation of the isotherm was obtained:

$$S_a = S_{o,a}\,(1 - C\,\ln\varphi)^{-1} \quad (8)$$

where $S_{o,a}$ is the maximum amount of water molecules absorbed by AD at φ=1, and coefficient $C=k\,S_{o,a}$. For C6P $S_{o,a}$ = 0.506 (g/g), while C =2.7.

The Equation (8) is similar to the equation presented in [19], which was derived from the Gibbs-Duhem relationship for the thermodynamic equilibrium in a binary sorbent-sorbate system.

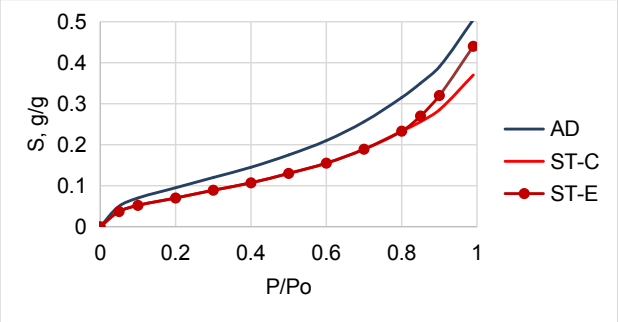

Figure 7. Calculated isotherms of WV for AD of C6P (AD) and sample of semicrystalline ST (ST-C); ST-E is experimental isotherm of ST sample

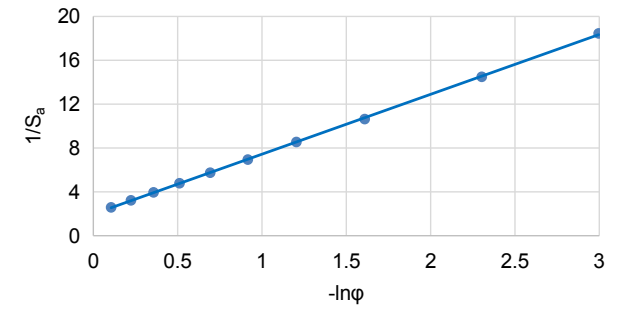

Figure 8. Linear form of sorption isotherm of WV for AD of C6P

To obtain the equation of sorption isotherm for a semicrystalline sample with a degree of amorphicity (Y), it is enough to introduce the Y-value in the Equation (8).

$$S = Y\,S_{o,a}\,(1 - C\,\ln\varphi)^{-1} \quad (9)$$

An example of the isotherm calculated for a semi-crystalline sample, ST-C, having Y = 0.72 is shown in Figure 7. The experimental isotherm of this sample, ST-E, is also presented. Comparison of the experimental and calculated isotherms for ST shows that in the φ-range from 0 to 0.8, these isotherms are practically identical. However, at $\varphi > 0.8$, a deviation of the experimental isotherm from the calculated one is observed. This phenomenon is caused by the known fact that at high relative vapor pressures, along with molecular sorption of water by polar groups of a low-porous hydrophilic polymer, also capillary condensation of WV occurs, which increases the amount of water in this polymer [16,30,31]. Using calculations by the Equation (9) it is possible to separate the molecularly sorbed water (Figure 7, red line) from the capillary water (Figure 7, brown line) at $\varphi > 0.8$.

3.4 Sorption of Water Vapor by Cellulose Samples and Other Unsubstituted Polysaccharides

The isotherms of WV sorption by semicrystalline cellulose samples have a sigmoid shape typical of hydrophilic biopolymers (Figure 9). To separate capillary-condensed water, the sections of isotherms above φ=0.8 were calculated using Equation (9). As a result, isotherms only molecularly sorbed water were obtained. Next, the isotherms also for other polysaccharides will include only molecularly sorbed water.

Studies have shown that the sorption ability (S) increases in direct proportion to the amorphicity degree (Y) of the sample (see e.g. Figure 10). Thus, it is confirmed that the process is performed via absorption of water molecules by amorphous domains of cellulose samples.

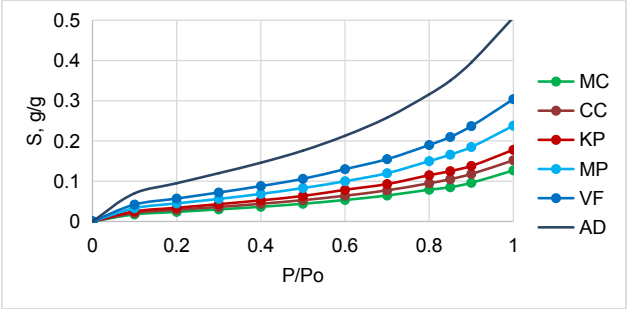

Figure 9. Sorption isotherms of WV for semicrystalline cellulose samples and AD of this biopolymer

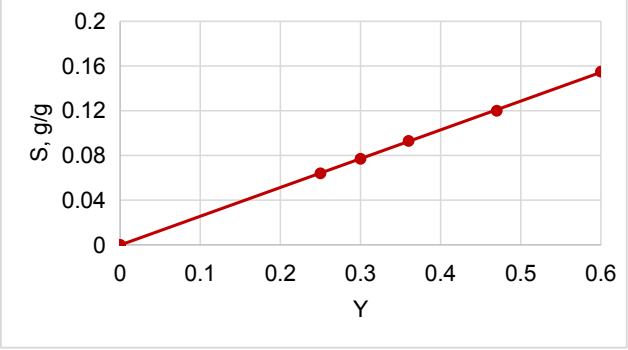

Figure 10. Dependence of sorption value at φ=0.7 on amorphicity degree of cellulose samples

If the sorption values at various φ to divide by the degree of amorphicity of the sample, then it is possible to obtain the sorption isotherm for AD that is general for all cellulose samples (Figure 9). This general isotherm is identical to AD isotherm in Figure 7 calculated by Equation (5) and (8) for AD of C6P, to which cellulose also belongs. This confirms the validity of the Van Krevelen method, on which these equations are based.

The sorption of WV by ST sample and its AD has been already discussed (see Figures 7 and 8). Another C6P biopolymer, such as MN, has sorption properties similar to ST.

Xylan, XL, belongs to C5P, therefore its sorption characteristics differ from those of biopolymers belonging to C6P. Since the repeating unit of isolated XL has only two OH-groups, the sorption capacity of its AD is lower than that AD of C6P, the repeating unit of which contains three OH-groups (Figure 11).

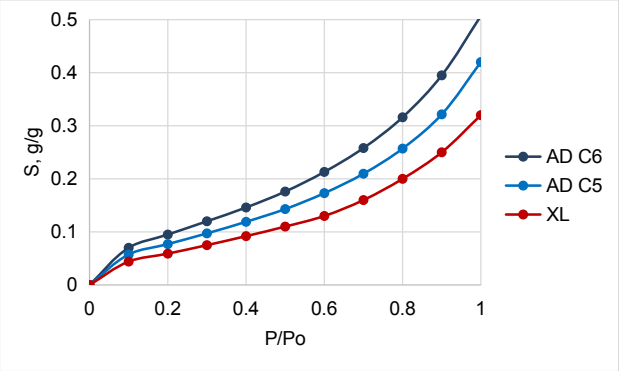

Figure 11. Sorption isotherms of WV for semicrystalline sample of isolated XL, AD of XL (AD C5) and AD of C6P (AD C6)

3.5 Sorption of Water Vapor by Substituted C6-polysaccharides

In this study, such substituted C6P as CT, CS, and PC were used. Since these samples were semicrystalline, their sorption values were understated (Figure 12).

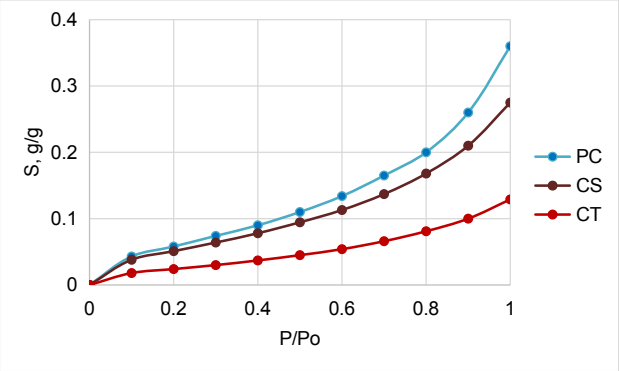

Figure 12. Sorption isotherms of WV by semicrystalline samples of PC, CS and CT

However, if consider sorption of WV by AD of these biopolymers, then the sorption capacity will be determined only by the type and content of polar groups. In the repeating unit of CS, one amino group substitutes one hydroxyl group at C2 present in C6P. The contribution of the amino group to sorption is close to the contribution of the hydroxyl group, therefore, the sorption isotherms for AD of CS and AD of C6P will be similar.

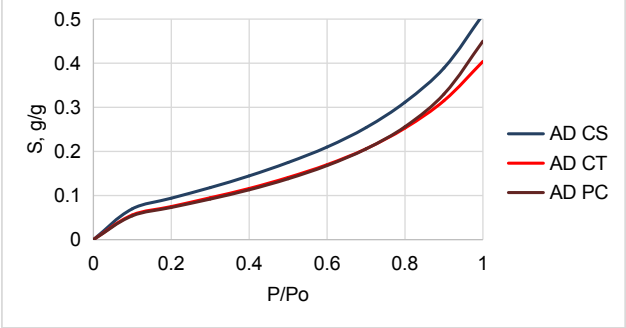

Figure 13. Sorption isotherms of WV for AD of CS (AD CS), CT (AD CT) and PT (AD PT)

Since the repeating unit of CT has a higher molecular weight than CS and contains low-polar acetyl groups, the sorption capacity for AD of CT will be lower than that for AD of CS and AD of C6P containing highly-polar amino- and hydroxyl groups. The same phenomenon is observed for AD of PC, the repeating unit of which contains a low-polar carboxyl group (Figure 13).

3.6 Enthalpy of Wetting

Calorimetric studies revealed (Table 5) that the interaction of various polysaccharides with water is accompanied by exothermic heat effects called the enthalpy of wetting ($\Delta_w H$).

Table 5. Enthalpy of wetting for samples of various polysaccharides

Sample	X	Y	$-\Delta_w H$, J/g
MC	0.75	0.25	42
CC	0.70	0.30	50
KP	0.64	0.36	61
MP	0.53	0.47	79
VF	0.36	0.64	108
ST	0.28	0.72	121
MN	0.26	0.74	124
XL	0.23	0.77	106
PC	0.20	0.80	118
CT	0.68	0.32	43
CS	0.46	0.54	92

For the same polysaccharide type, e.g. C6P, samples of which have different crystallinity and amorphicity, the enthalpy of wetting is directly proportional to the

amorphicity degree (Figure 14).

Such dependence confirms that the interaction occurs by volume absorption of water in AD of the polysaccharides. The slope factor of the straight line in Figure 14 gives the value $\Delta_w H_a$ = -168 (J/g), which is the wetting enthalpy of the amorphous phase of C6P.

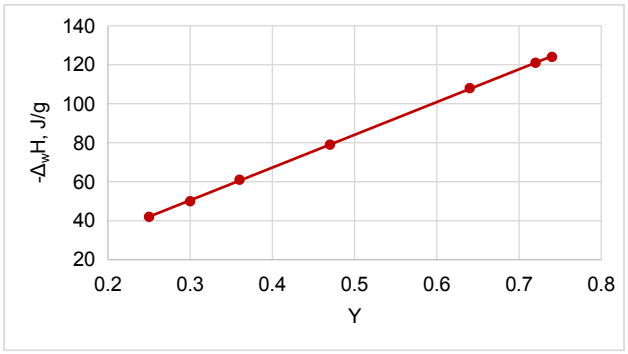

Figure 14. Dependence of enthalpy of wetting on amorphicity degree for samples of C6P

Values of $\Delta_w H_a$ for other samples can be found by dividing the experimental value of the wetting enthalpy for the sample by its amorphicity degree (Table 6).

4. Discussion

To describe the sorption isotherms of water vapor for hydrophilic biopolymers, including polysaccharides, the equations of multilayer surface adsorption such as BET and GAP are mostly used in the literature [10-13,16,32-34]. Using these equations, the value of the monolayer adsorption, specific surface area, and the constants of these equations are calculated. However, it has been proven that polysaccharides and other hydrophilic biopolymers interact with water by the absorption mechanism. Therefore, the calculations of adsorption characteristics for absorbing sorbents using BET or GAP equations have no physical meaning.

To describe the absorption process, the Flory-Rehner, Hailwood Horrobin, and some other equations can be used [16]. However, the studies revealed that the best conformity with experiments gives the use of the equation of type (9): $S = Y\ S_{o,a}\ (1 - C\ \ln\varphi)^{-1}$, parameters of which for samples of various polysaccharides are presented in Table 6.

Table 6. Parameters of Equation (9)

Polysaccharides	C	$S_{o,a}$, g/g	$-\Delta_w H_a$, J/g
C5P	2.7	0.410	137
C6P	2.7	0.506	168
CS	2.7	0.510	170
CT	2.7	0.400	134
PT	3.1	0.440	147

It has been found that crystallinity strongly affects the sorption capacity and wetting enthalpy. Therefore, to compare the hydrophilicity of various polysaccharides with different crystallinity, it is necessary to use hydrophilic characteristics of amorphous domains of semicrystalline biopolymers. After that, the relative hydrophilicity index (HI) of various polysaccharides can be calculated. For this purpose, the following ratios were calculation:

$$HI_s = S_{o,a}(P)/S_{o,a}(C6P) \text{ and } HI_e = \Delta_w H_a(P)/\Delta_w H_a(C6P) \quad (10)$$

where HI_s and HI_e are hydrophilicity indexes measured by sorption, and wetting enthalpy, respectively; $S_{o,a}(P)$ and $S_{o,a}(C6P)$ are maximum sorption values for AD of tested polysaccharide (P), and C6P, respectively; $\Delta_w H_a(P)$ and $\Delta_w H_a(C6P)$ are wetting enthalpies for AD of tested polysaccharide (P), and C6P, respectively.

The calculations showed that the values of HI_s and HI_e are equal; therefore, the common hydrophilicity index (HI) was subsequently used. As follows from Figure 15, chitosan is the most hydrophilic polysaccharide type among the studied biopolymers, while other substituted polysaccharides, pectin, xylan, and chitin showed less hydrophilicity.

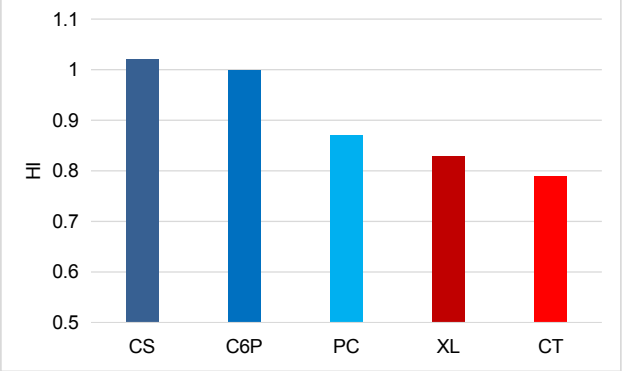

Figure 15. Hydrophilicity index of various polysaccharides

Since the contribution of the amino group of chitosan and the hydroxyl group of C6-polysaccharides to sorption are close, it can be expected that the HI for CS and C6P will be similar. However, in reality, the HI for CS is slightly higher than for C6P. This can be explained by the fact that the binding energy of water molecules with the nitrogen atoms of the amino groups of CS is greater than with the oxygen atoms of hydroxyl groups of C6P [35].

The decreased HI for PC, XL, and CT is because repeating units of these polysaccharides contain two unsubstituted hydroxyl groups instead of three in C6P. An additional reason for the low HI of CT is that, firstly, repeating unit

of this biopolymer contains a low-polar acetyl group; and secondly, the molecular weight (MW) of the repeating unit of CT is the largest of all the studied polysaccharides (Table 3), thus relative sorption value expressed in gram H_2O per gram biopolymer will be the smallest.

Discussing the process of water vapor sorption by polysaccharides, an additional problem arises because the amorphous domains of all these biopolymers are in a glassy state at room temperature. Since all these polymers are low-porous, then theoretically the sorption of water vapor in glassy AD of the biopolymers at the low and middle φ-ranges should be absent, and begins only at increased vapor pressures, when as a result of the plasticizing action of water the glass transition temperatures decrease below the temperature of sorption experiment, 25 °C. However, the experiments do not support this theory, which requires an explanation.

The explanation is that amorphous domains of biopolymers have heterogeneous packing since they consist of clusters with different packing densities and energies of hydrogen bonds [36]. Despite the glassy state of densely packed clusters, in less densely packed clusters, local mobility of small segments is possible, which creates a free volume sufficient for the penetration of small water molecules. For example, it was calculated that the free volume of loosely packed clusters in AD of such C6P as cellulose is $V_f = 3.32 \times 10^{-23}$ cm^3 per one monomeric unit, which exceeds the volume of a water molecule, $V_w = 2.99 \times 10^{-23}$ cm^3.

As a result, at the initial sorption stage, water molecules can penetrate in loosely packed clusters of AD and intensively sorb by polar groups of these clusters. This initial sorption stage is accompanied by a high exothermic heat effect [16]. The beginning sorption leads to a weakening of the H-bonds of neighboring clusters, which promotes further gradual sorption of water molecules at the middle φ-range. This process continues until the densely packed clusters soften at increased relative vapor pressures due to the plasticizing effect of the absorbed water, which leads to a sharp increase in further sorption of water vapor at $\varphi > 0.8$ [16,36].

When the polysaccharides are wetted with water, their amorphous domains soften and pass into a viscoelastic state, which provides fast and complete absorption of water molecules in AD accompanied by an exothermal wetting effect, i.e. enthalpy.

5. Conclusions

The specific surface area, sorption of water vapor, and wetting enthalpy of various polysaccharides (cellulose, hemicelluloses, starch, pectin, chitin, and chitosan) have been studied. It was found that the specific surface area of the dry samples measured by sorption of inert vapor of n-hexane was low indicates the low-porous structure of these polysaccharides. As opposite, the specific surface area measured by sorption of active water vapor was 20-80 times higher and correlates with the amorphicity degree of the samples. It was shown that crystallites are inaccessible for water, and therefore water molecules can interact only with polar groups in noncrystalline (amorphous) domains of biopolymers. The isotherms of water vapor sorption for various polysaccharides had sigmoid shapes, which can be explained by the absorption of water molecules in heterogeneous amorphous domains having clusters with different packing densities. The method of contributions of polar groups to sorption of water molecules was used, which allowed to derivate a simple calculating equation to describe the shape of sorption isotherms. The wetting of biopolymers with water was accompanied by a high exothermic thermal effect, in direct proportion to the amorphicity degree. The sorption values and wetting enthalpies of amorphous domains of biopolymers were calculated, which allowed to find the hydrophilicity index and comparing the hydrophilicity of the various polysaccharides. The calculations showed that the amino-polysaccharide, chitosan, is the most hydrophilic among the studied biopolymers, while other substituted polysaccharides, pectin xylan, and chitin are characterized by reduced hydrophilicity.

References

[1] Thomas, S., Ninan, N., Mohan, S., Francis, E., 2012. Natural Polymers, Biopolymers, Biomaterials, and Their Composites, Blends, and IPNs. Academic Press: New York. pp. 444.

[2] John, M.J., Thomas, S., 2012. Natural Polymers. RCS Publishing: Landon. pp. 313.

[3] Kantappa, H., Kim, H.J., Birajdar, M., et al., 2016. Recently developed applications for natural hydrophilic polymers. J. Ind. Eng. Chem. 40, 16-22. DOI: https://doi.org/10.1016/j.jiec.2016.06.01.

[4] Ioelovich, M., 2021. Adjustment of hydrophobic properties of cellulose materials. Polymers. 13(8), 1241-1252. DOI: https://doi.org/10.3390/polym13081241.

[5] Scheller, H.V., Ulvskov, P., 2010. Hemicelluloses. Ann. Rev. Plant. Biol. 61, 263-89. DOI: https://doi.org/10.1146/annurev-arplant-042809-112315.

[6] Cornejo-Ramírez, Y.I., Martínez-Cruz, O., Del Toro-Sánchez, C.L., et al., 2018. The structural char-

acteristics of starches and their functional properties, CyTA - Journal of Food. 16(1), 1003-1017. DOI: https://doi.org/10.1080/19476337.2018.1518343.

[7] Elieh-Ali-Komi, D., Hamblin, M.R., 2016. Chitin and Chitosan: Production and Application. Int. J. Adv. Res. 4(3), 411-427.

[8] Marmur, A., 2009. Solid surface characterization by wetting. Ann. Rev. Mater. Res. 39(1), 473-489. DOI: https://doi.org/10.1146/annurev.matsci.38.060407.132425.

[9] El-Saftawy, A.A., Abd El Aal, S.A., Badawy, Z.M., Soliman, B.A., 2014. Investigating wettability and optical properties of PADC polymer irradiated by low energy Ar ions. Surface and Coatings Technol. 253, 249-254. DOI: https://doi.org/10.1016/j.surfcoat.2014.05.048.

[10] Timmermann, E.O., 2003. Multilayer sorption parameters: BET or GAB values. Colloid Surface A. 220, 235-260. DOI: https://doi.org/10.1016/S0927-7757(03)00059-1.

[11] Czepirsky, L., Komarowska-Czepirska, E., Szymonska, J., 2002. Fitting of different models for water vapor sorption on potato starch granules. Appl. Surface Sci. 196(1-4), 150-153. DOI: https://doi.org/10.1016/S0169-4332(02)00050-8.

[12] Brousse, M.M., Linares, R.A., Vergara, M.L., Nieto, A.B., 2017. Adsorption isotherm of dehydrated mashed cassava from different varieties. RECyT. 19(28), 29-37.

[13] Blahovec, J., Yanniotis, S., 2008. GAB generalized equation for sorption phenomena. Food Bioprocess Technol. 1, 82-90. DOI: https://doi.org/10.1007/s11947-007-0012-3.

[14] Park, G.S., 1986. Transport Principles-Solution, Diffusion and Permeation in Polymer Membranes. In: Bungay P.M., Lonsdale H.K., de Pinho M.N. (eds) Synthetic Membranes: Science, Engineering and Applications. NATO ASI Series C: Mathematical and Physical Sciences, vol 181. Springer: Dordrecht. pp. 57-108.

[15] Bessadok, A., Langevin, D., Gouanvé, F., et al., 2009. Study of water sorption on modified Agave fibres. Carbohyd. Polym. 76, 74-85. DOI: https://doi.org/10.1016/j.carbpol.2008.09.033.

[16] Papkov, S.P., Fainberg, E.Z., 1976. Interaction of Cellulose and Cellulosic Materials with Water. Chemistry: Moscow. pp. 232.

[17] Zografia, G., Kontnya, M.J., Yangb, A.Y.S., Brennerb, G.S., 1984. Surface area and water vapor sorption of microcrystalline cellulose. Int. J. Pharmac. 18(1-2), 99-116. DOI: https://doi.org/10.1016/0378-5173(84)90111-X.

[18] Ioelovich, M., 2009. Accessibility and crystallinity of cellulose. Bioresources. 4(3), 1168-1177. DOI: https://doi.org/10.15376/BIORES.4.3.1168-1177.

[19] Ioelovich, M., Leykin, A., 2011. Study of sorption properties of cellulose and its derivatives. Bioresorces. 6(1), 178-195. DOI: https://doi.org/10.15376/biores.6.1.178-195.

[20] Hill, C.A.S., Norton, A., Newman, G., 2009. The water vapor sorption behavior of natural fibers. J. Appl. Polym. Sci. 112, 1524-1537. DOI: https://doi.org/10.1002/app.29725.

[21] Bismarck, A., Aranberri-Askargorta, I., Springer, J., et al., 2002. Surface characterization of flax, hemp and cellulose fibers; surface properties and the water uptake behavior. Polymer composites. 23(5), 872-894. DOI: https://doi.org/10.1002/pc.10485.

[22] Chirkova, J., Andersons, B., Andersone, I., 2007. Study of the structure of wood-related biopolymers by sorption methods. Bioresources. 4(3), 1044-1057.

[23] Takur, V.K., Takur, M.K., 2016. Handbook of Sustainable Polymers: Structure and Chemistry. PAN Stanford Publ: New York. pp. 988.

[24] Ago, M., Endo, T., Hirotsu, T., 2004. Crystalline transformation of native cellulose from cellulose I to cellulose II polymorph by a ball milling method with a specific amount of water. Cellulose. 11(2), 163-167. DOI: https://doi.org/10.1023/B:CELL.0000025423.32330.fa.

[25] Paes, S.S., Sun, Sh., MacNaughtan, W., et al., 2010. The glass transition and crystallization of ball milled cellulose. Cellulose. 17(4), 693-709. DOI: https://doi.org/10.1007/s10570-010-9425-7.

[26] Ioelovich, M., 2016. Physico-chemical methods for determination of cellulose crystallinity. ChemXpress. 9(3), 245-251.

[27] Ioelovich, M., 2016. Models of supramolecular structure and properties of cellulose. Polymer Sci. A. 58(6), 925-943. DOI: https://doi.org/10.1134/S0965545X16060109.

[28] Ioelovich, M., 2016. Study of thermodynamic properties of various allomorphs of cellulose. ChemXpress. 9(3), 259-265.

[29] Van Krevelen, D.W., Nijenhuis, K., 2009. Properties of Polymers: Correlations with Chemical Structure. Elsevier: Amsterdam. pp. 1004.

[30] Engelund, E.T., 2011. Wood - water interactions: Linking molecular level mechanisms with macroscopic performance. University Press: Copenhagen. pp. 171.

[31] Shi, J., Avramidis, S., 2017. Water sorption hysteresis in wood: III physical modeling by molecular simulation. Holzforschung. 71, 733-741.
DOI: https://doi.org/10.1515/hf-2016-0231.

[32] Agrawal, A.M., Manek, R.V., Kolling, W.M., Neau, S.H., 2004. Water distribution studies within microcrystalline cellulose and chitosan using differential scanning calorimetry and dynamic vapor sorption analysis. J. Pharma. Sci. 93(7), 1766-1779.
DOI: https://doi.org/10.1002/jps.20085.

[33] Manek, R.V., Builders, P.F., Kolling, W.M., et al., 2012. Physicochemical and binder properties of starch obtained from *Cyperus esculentus*. AAPS Pharm. Sci. Tech. 13(2), 379-388.
DOI: https://doi.org/10.1208/s12249-012-9761-z.

[34] Bertolin, Ch., Ferri, L., Strojecki, M., 2020. Application of the Guggenheim, Anderson, de Boer (GAB) equation to sealing treatments on pine wood. Proc. Struct. Integ. 26, 147-154.
DOI: https://doi.org/10.1016/j.prostr.2020.06.018.

[35] Grinberg, N., Grushka, E., 2018. Advances in Chromatography. Vol. 54. CRC Press: Boca Raton. pp. 182.

[36] Ioelovich, M., 2016. Isophase transitions of cellulose - A short review. Athens J. Sci. 3(4), 309-322.

BILINGUAL PUBLISHING CO.
Pioneer of Global Academics Since 1984

Organic Polymer Material Research
https://ojs.bilpublishing.com/index.php/opmr

EDITORIAL

Organic Polymer Materials for Light Emitting Diode Applications

Fayroz Arif Sabah*

Department of Medical Instrumentation Engineering Techniques, College of Medical Techniques, Alfarahidi University, Baghdad, Iraq

ARTICLE INFO

Article history
Received: 27 December 2021
Accepted: 10 January 2022
Published Online: 18 January 2022

There are two common types of polymers (thermoplastics and thermosets), which have been classified by various methods depending on their molecular structures. The bonding of molecular chains is the fundamental physical difference between these two polymer types. The polymer types are named based on their general thermal and processing characteristics, and chemical structure, which in turn significantly influence their polymer properties [1].

Thermoplastics have secondary bonds between molecular chains, low melting points and low tensile strength, and are lower in molecular weight compared to thermosetting plastics. While, thermosetting plastics have primary bonds between molecular chains, held together by strong cross-links, have high melting points and tensile strength, and are high in molecular weight [2,3]. Thermoplastic composites can be reconfigured/repaired unlike thermosetting composites when applying heat and this cycle can be frequent. In terms of impact resistance, thermoplastic polymers exhibit good elastic-plastic behaviour and thus have better impact performance than their thermosetting counterparts [4,5]. All thermoplastic materials exist in any of the three polymer phases depending on the changes in temperature used [1]. Thermosetting polymers are based on epoxies, polyesters, polyimides and phenolics [6], and mostly exist only in the initial two phases [1].

Polyvinyl alcohol (PVA) is a hydrophilic polymer [7] that is valuable in material studies and practical applications by reason of its physical properties. PVA is a linear polymer with formula $[CH_2CH(OH)]_n$ [8]. PVA hydrogel is characterized by a noncorrosive nature, easy synthesis and amenability, high transmittance and good thermal stability over a wide temperature range, and typical matrix for optoelectronic applications [7].

**Corresponding Author:*
Fayroz Arif Sabah,
Department of Medical Instrumentation Engineering Techniques, College of Medical Techniques, Alfarahidi University, Baghdad, Iraq
Email: fayroz.arif@gmail.com

DOI: https://doi.org/10.30564/opmr.v3i2.4348

PVA is applied in the production of catalyst pellets, cork compositions, binders in fibers, pigments, ceramics, plastics, cement, etc. In addition, PVA has garnered interest in biomedical applications. However, PVA is unstable when subjected to heat treatment mostly near melting point. This instability due to the inherent presence of hydroxyl groups makes its melting point close to the glass transition temperature [8].

In recent time, polymers and semiconductors (with built in nanocomposite structures) have attracted attention in the field of material science due to their ability to modify the physicochemical properties of the materials. Nano-sized particles improve their optoelectronic properties, by facilitating the coupling of mechanical and optoelectronic properties. Polymer matrix composite enhances the growth, long shelf life, and stability of the nanoparticles in addition to inhibiting their aggregation. Factors that directly affect the properties of particulate polymer nanostructure include particle concentration, size, shape, the method of dispersing particles, and their interaction with the polymer matrix [7].

References

[1] Brinson, H.F., Brinson, L.C., 2008. Characteristics, Applications and properties of polymers, in: Polymer Engineering Science and Viscoelasticity: an Introduction. Springer US, Boston, MA. pp. 55-97.

[2] https://byjus.com/chemistry/difference-between-thermoplastic-and-thermosett ing-plastic/.

[3] Zhang, J., de Souza, M., Creighton, C., Varley, R.J., 2020. New approaches to bonding thermoplastic and thermoset polymer composites. Compos. Appl. Sci. Manuf. 105870.

[4] Pinto, D.G., Rodrigues, J., Bernardo, L., 2020. A review on thermoplastic or thermosetting polymeric matrices used in polymeric composites manufactured with banana fibers from the pseudostem. Appl. Sci. 10, 3023.

[5] Jogur, G., Nawaz Khan, A., Das, A., Mahajan, P., Alagirusamy, R., 2018. Impact properties of thermoplastic composites, Textil. Prog. 50, 109-183.

[6] Liao, H.K., Wu, C.L., Chou, J.C., Chung, W.Y., Sun, T.P., Hsiung, S.K., 1999. Multi-structure ion sensitive field effect transistor with a metal light shield. Sensor. Actuator. B Chem. 61, 1-5.

[7] Yadav, S., Bajpai, P.K., 2018. Effect of substrate on Cus/Pva nanocomposite thin films deposited on glass and silicon substrate. Soft. Nanosci. Lett. 8, 9.

[8] Salman, S., Bakr, N., Humad, H.T., 2018. Section C: physical sciences DSC and TGA properties of PVA films filled with Na2S2O35H2O salt. J. Chem. Biol. Phys. Sci. 8, 001-011.

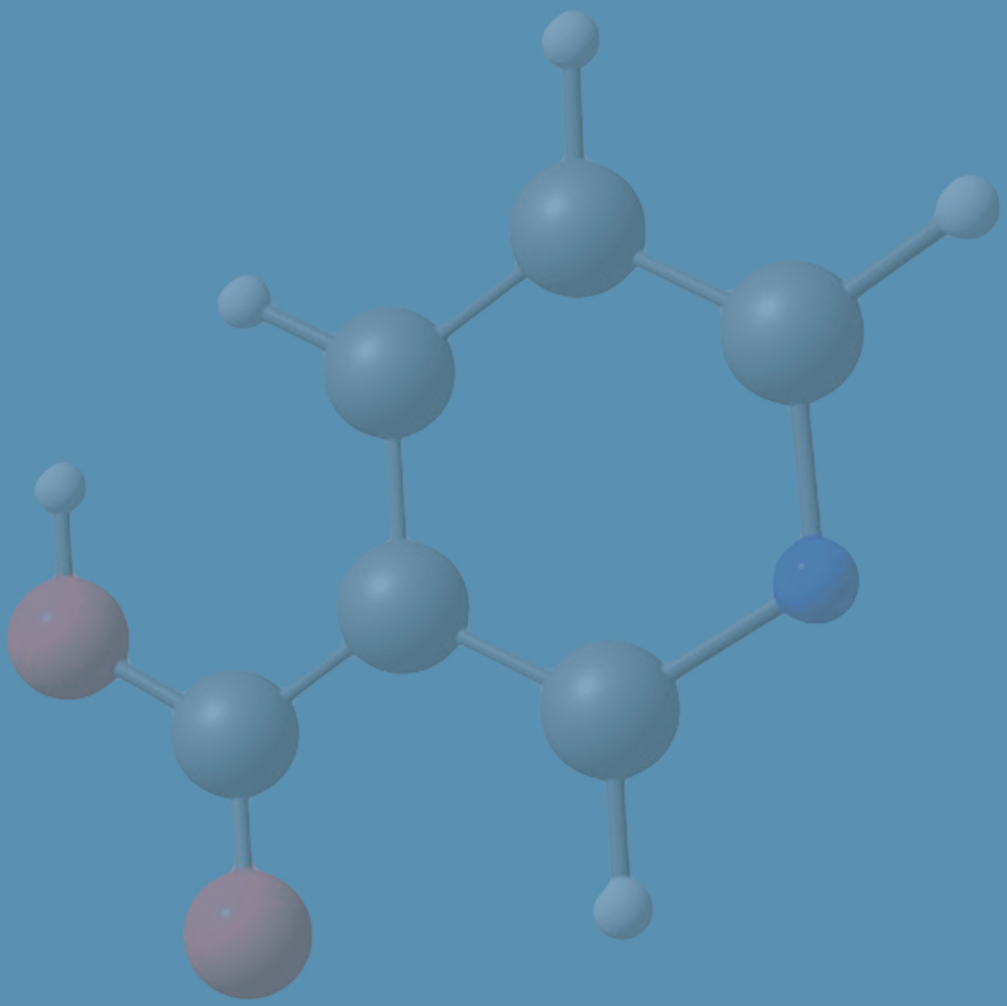

BILINGUAL
PUBLISHING CO.
Pioneer of Global Academics Since 1984

Tel:+65 65881289
E-mail: contact@bilpublishing.com
Website:ojs.bilpublishing.com

2661-3875
02
9 772661 387219